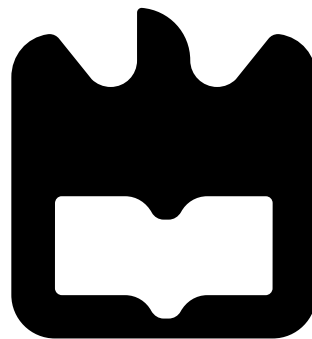




**João Nuno  
Oliveira Ramos da  
Silva**

**Projecto de um Amplificador de Potência para o  
standard IEEE 802.11p**

**Design of a Power Amplifier for IEEE 802.11p  
Applications**







**João Nuno  
Oliveira Ramos da  
Silva**

**Projecto de um Amplificador de Potência para o  
standard IEEE 802.11p**

**Design of a Power Amplifier for IEEE 802.11p  
Applications**

Dissertação apresentada à Universidade de Aveiro para cumprimento dos requisitos necessários à obtenção do grau de Mestrado Integrado em Engenharia Electrónica e Telecomunicações, realizada sob a orientação científica do Dr. João Nuno Pimentel da Silva Matos, Professor Associado do Departamento de Electrónica, Telecomunicações e Informática da Universidade de Aveiro, e sob a co-orientação científica do Dr. Arnaldo Silva Rodrigues de Oliveira, Professor Auxiliar do Departamento de Electrónica, Telecomunicações e Informática da Universidade de Aveiro.



**Dedicatória**

Dedico este trabalho à minha família, à minha namorada e ao meu falecido bisavô.



**o júri / the jury**

presidente / president

**Prof. Dr. José Carlos Esteves Duarte Pedro**

Professor Catedrático da Universidade de Aveiro (por delegação da Reitora da Universidade de Aveiro)

vogais / examiners committee

**Prof. Dr. João Nuno Pimentel da Silva Matos**

Professor Associado da Universidade de Aveiro (orientador)

**Prof. Dr. João Manuel Torres Caldinhas Simões Vaz**

Professor Auxiliar do Instituto Superior Técnico (arguente)





## **agradecimentos / acknowledgements**

Agradeço, em primeiro lugar, aos meus pais, que permitiram a realização dos meus estudos e suportaram todos os bons e maus momentos durante os últimos 5 anos, especialmente nos últimos meses.

À Ana pela sua presença e apoio nos dias complicados, assim como nos momentos de descontração e lazer. Gostaria também de estender o agradecimento aos meus amigos mais próximos tanto do universo universitário como basquetebolístico, em especial, ao Gonçalo, Lopes, Jaime e Hugo.

Ao meu orientador Professor João Nuno Matos pelo apoio, discussões e conhecimento transmitido. Ao Mestre Luís Cótimos, ao Mestre Filipe Barradas e ao Mestre André Prata pela ajuda essencial em alguns momentos do trabalho desenvolvido.

Ao Paulo Gonçalves pela grande ajuda nas montagens e impressão das placas de circuito impresso necessárias à realização deste trabalho.

Ao Instituto de Telecomunicações pelas excelentes condições proporcionadas para a realização deste trabalho.

A todos os mencionados anteriormente e a alguém que me possa ter esquecido, o meu sincero Obrigado!



## Palavras Chave

amplificadores, classes de operação, pré-distorção digital, DSRC, eficiência, ITS, linearidade, polinómio com memória, potência, rádio frequência, comunicações veiculares

## Resumo

Comunicações veiculares em Dedicated Short Range Communications (DSRC) e Intelligent Transportation Systems (ITS) são cada vez mais comuns e usadas no dia a dia. Para este tipo de comunicações funcionar, um standard foi desenvolvido através de melhorias do usado regularmente em Wi-Fi, o IEEE 802.11p, que funciona na banda dos 5.9 GHz. De forma a permitir o uso deste tipo de sistemas de comunicação, os Amplificadores de Potência são uma das partes importantes dos front-ends de RF. Estes devem ser o mais linear possível para que seja possível atingir elevadas taxas de transmissão de dados e cumprir com a Máscara Espectral de Emissão. A linearidade pode ser alcançada pela escolha correcta do ponto de polarização do transistor ou através de pré-distorção. Como a eficiência é também uma das maiores preocupações nos sistemas de comunicação actuais, as técnicas de pré-distorção são cada vez mais usadas, evitado assim um back-off desnecessário do amplificador de potência.

Nesta dissertação, o objectivo é desenhar e implementar um amplificador de potência que possa ser utilizado nas quatro classes de potência definidas pelo standard IEEE 802.11p: A, B, C e D, sendo a D a mais restritiva, que requer um amplificador altamente linear. Para que este objectivo possa ser cumprido, alguns conceitos teóricos são explicados durante esta dissertação sobre o standard e características relacionadas com amplificadores de potência. O design e simulação são apresentados com várias ilustrações e resultados para descrever todo o trabalho realizado de forma coerente e simples, desde o design do amplificador de potência até à implementação do pré-distorçor digital. Enquanto que para as classes A, B e C o amplificador desenhado cumpre as especificações, para a classe D recorreu-se a um pré-distorçor digital. No fim deste documento, o amplificador é testado com e sem pré-distorção, comparando ambos os resultados, assim como são feitos testes com 1-tom para análise da eficiência, ganho e potência de saída para a frequência de operação do standard IEEE 802.11p. Uma análise crítica e propostas de trabalho futuro são apresentadas como nota final desta dissertação.



**Keywords**

amplifiers, classes of operation, digital predistortion, DSRC, efficiency, ITS, linearity, memory polynomial, power, radio frequency, vehicular communications

**Abstract**

Vehicular communications in Dedicated Short Range Communications (DSRC) and Intelligent Transportation Systems (ITS) are becoming more common and used nowadays. For this type of communications to work a standard was developed as an improvement from the Wi-Fi regular standard, the IEEE 802.11p, that works in the 5.9 GHz band. In order to allow the use of such communication systems, Power Amplifiers (PAs) are one of the most important parts of the RF front-ends. They have to be as linear as possible to allow high transmission data rates and Spectrum Emission Mask (SEM) compliance. Linearity can be achieved through the correct selection of the transistor bias point or through predistortion. Since efficiency is also one of the main concerns for today's communication systems, predistortion is becoming a technique that is commonly used, avoiding an unnecessary back-off of the PA.

In this thesis, the objective is to design and implement a PA that is compliant with the four power classes of the IEEE 802.11p standard: A, B, C and D, being D the most stringent one, which requires a highly linear amplifier. In order to achieve this goal, some theoretical concepts are explained during this thesis, regarding the standard and PA characteristics.

The design and simulation are presented with several illustrations and results to sustain and describe all the work performed in a cohesive and simple way, from the PA design to the Digital Predistorter (PD) implementation. While for classes A, B and C the designed amplifier matches the specifications, for class D a Digital PD was used.

In the end of this document, the PA is tested with and without the PD, comparing both results and also doing the regular 1-tone tests for efficiency, gain and power output for the frequency of operation of the IEEE 802.11p standard. A critical analysis and future work are presented as a last remark of this thesis.



# Contents

<b>Contents</b>	<b>i</b>
<b>List of Figures</b>	<b>v</b>
<b>List of Tables</b>	<b>vii</b>
<b>Acronyms</b>	<b>ix</b>
<b>1 Introduction</b>	<b>1</b>
1.1 Motivation . . . . .	1
1.2 Objectives and Contributions . . . . .	2
1.3 Structure . . . . .	3
<b>2 Framework</b>	<b>5</b>
2.1 Vehicular Communications . . . . .	5
2.1.1 IEEE 802.11p . . . . .	6
2.1.2 Orthogonal Frequency Division Multiplexing . . . . .	7
<b>3 Power Amplifiers</b>	<b>11</b>
3.1 Introduction . . . . .	11
3.2 S-Parameters . . . . .	11
3.3 Bias Point and Classes of Operation . . . . .	13
3.4 Linearity . . . . .	17
3.4.1 Linear and Non-Linear Systems . . . . .	17
3.4.2 Linearity in Power Amplifiers . . . . .	17
3.5 1dB Compression Point . . . . .	18
3.6 3rd Order Interception point . . . . .	19
3.7 Efficiency . . . . .	19

3.7.1	Power Added Efficiency . . . . .	20
3.8	Adjacent Channel Power Ratio (ACPR) . . . . .	21
3.9	Stability . . . . .	21
3.10	Technologies . . . . .	23
<b>4</b>	<b>Power Amplifier Design</b>	<b>25</b>
4.1	Transistor and Substrate . . . . .	25
4.2	Bias Point . . . . .	26
4.3	Load-Pull . . . . .	27
4.4	Source-Pull . . . . .	29
4.5	Bias Network . . . . .	31
4.6	Impedance Matching Networks and Stability . . . . .	35
4.6.1	Capacitors . . . . .	35
4.6.2	Output IMN . . . . .	35
4.6.3	Stability . . . . .	37
4.6.4	Input IMN . . . . .	37
4.7	Minor Adjustments and Optimizations . . . . .	39
<b>5</b>	<b>Simulation Results</b>	<b>45</b>
5.1	1-Tone simulation with Ideal Components . . . . .	45
5.2	1-Tone Simulation with MoM models . . . . .	46
5.3	2-Tone Simulation with MoM Models . . . . .	46
5.4	Stability Simulations . . . . .	48
<b>6</b>	<b>Digital Pre-Distortion</b>	<b>51</b>
6.1	Introduction . . . . .	51
6.2	Why use Digital Pre-Distortion? . . . . .	51
6.2.1	Polynomial model with memory . . . . .	53
6.3	Polynomial Model with memory of a Digital Predistorter (PD) . . . . .	54
6.4	Polynomial model with memory of the Digital PD using Matlab . . . . .	55
6.5	DPD Results . . . . .	56
<b>7</b>	<b>Results</b>	<b>61</b>
7.1	Setup and PA built . . . . .	61
7.2	1-Tone Measurements . . . . .	61
7.3	IEEE 802.11p measurements . . . . .	63



<b>8</b>	<b>Conclusions and Future Work</b>	<b>67</b>
8.1	Summary and Conclusions . . . . .	67
8.2	Future Work . . . . .	69
	<b>Bibliography</b>	<b>71</b>



# List of Figures

1.1	Electromagnetic Spectrum Distribution . . . . .	2
2.1	Example of the distribution of sub-carriers in FDMA . . . . .	8
2.2	Use of Guard Interval to prevent ISI . . . . .	8
2.3	Sinc function representation in a OFDM application . . . . .	9
2.4	Representation of an OFDM system . . . . .	9
3.1	Representation of a two-port network . . . . .	12
3.2	Representation of a two-port network using Voltages and Currents . . . . .	13
3.3	Class A conduction angle . . . . .	14
3.4	Class B conduction angle . . . . .	15
3.5	Class AB conduction angle . . . . .	15
3.6	Class C conduction angle . . . . .	16
3.7	Class F conduction angle . . . . .	16
3.8	AM-AM and AM-PM curves . . . . .	18
3.9	Power Output versus Input Power in a PA . . . . .	19
3.10	Representation of the 3rd Order Interception Point . . . . .	20
3.11	Representation of the ACPR effect due to non-linearities . . . . .	21
3.12	Transistor cut-off frequency comparison for various device technologies . . . . .	24
4.1	CREE CGH55015 transistor . . . . .	26
4.2	Setup for DC bias . . . . .	27
4.3	Choice of Bias Point for the PA . . . . .	28
4.4	Setup for Load-Pull . . . . .	29
4.5	Load-Pull results . . . . .	29
4.6	Source Impedance seen at the gate of the transistor . . . . .	30
4.7	Smith Chart quarter lambda transformer . . . . .	32

4.8	Input Bias Network . . . . .	33
4.9	Output Bias Network . . . . .	34
4.10	Impedance of the capacitor between 1 and 10 Ghz . . . . .	36
4.11	Output IMN schematic . . . . .	38
4.12	Output IMN Smith Chart . . . . .	39
4.13	Input IMN Schematic . . . . .	40
4.14	Input IMN Smith Chart . . . . .	41
4.15	Final Layout without components . . . . .	42
5.1	1-tone Simulation with ideal components . . . . .	45
5.2	Results of 1-tone Simulation with ideal components . . . . .	45
5.3	1-tone Simulation Results . . . . .	47
5.4	2-tone Simulation Results . . . . .	47
5.5	2-tone Simulation Results . . . . .	48
5.6	Stability Simulations . . . . .	49
6.1	Schematic of Digital Pre-Distortion (DPD) use with a PA . . . . .	51
6.2	DPD example and obtained results . . . . .	52
6.3	PD calculation using direct learning . . . . .	54
6.4	Setup used for measurements . . . . .	55
6.5	NMSE values for different M and K . . . . .	57
6.6	Comparison of a signal with PD and without PD . . . . .	57
6.7	EVM analysis of a 16-QAM signal without DPD . . . . .	58
6.8	EVM analysis of a 16-QAM signal with DPD . . . . .	59
6.9	Comparison of a signal with PD and without PD before PA. . . . .	59
7.1	Class AB GaN HEMT PA for IEEE 802.11p applications - 5.9 GHz . . . . .	62
7.2	Gain, output power and Power Added Efficiency (PAE) measurements . . . . .	62
7.3	Power spectrum of the signal compared to SEM of power class C . . . . .	64
7.4	Channel power for the signal compliant with the SEM of power class C . . . . .	65
7.5	Power spectrum of the signal compared to SEM of power class D . . . . .	65
7.6	Power spectrum of the signal with PD compared to SEM of power class C . . . . .	66
7.7	Power spectrum of the signal with PD compared to SEM of power class D . . . . .	66

# List of Tables

2.1	Maximum Transmitted Power for DSRC Band . . . . .	7
2.2	Transmitted Spectrum Mask for 10 MHz Channels . . . . .	7
3.1	Characteristics of each Bias point using conduction angle . . . . .	16
4.1	Rogers 4350B substrate characteristics . . . . .	27
7.1	Comparison between the simulated and the experimental results of the PA	63



# Acronyms

<b>ACPR</b>	Adjacent Channel Power Ratio
<b>ADS</b>	Advanced Design System
<b>BJT</b>	Bipolar Junction Transistor
<b>CAD</b>	Computer Aided Design
<b>DPD</b>	Digital Pre-Distortion
<b>DSRC</b>	Dedicated Short Range Communications
<b>EVM</b>	Error Vector Magnitude
<b>FDMA</b>	Frequency Division Multiple Access
<b>GaN</b>	Gallium Nitride
<b>GaAsFET</b>	Gallium Arsenide Field effect Transistor
<b>GSM</b>	Global System for Mobile Communications
<b>GPS</b>	Global Positioning System
<b>HEMT</b>	High electron mobility Transistor
<b>IMN</b>	Impedance Matching Network
<b>IP3</b>	Third order Interception Point
<b>ISI</b>	Inter Symbol Interference
<b>ITS</b>	Intelligent Transportation Systems

<b>JFET</b>	Junction Gate Field effect Transistor
<b>LTE</b>	Long Term Evolution
<b>MESFET</b>	Metal Semiconductor Field effect Transistor
<b>MMIC</b>	Monolithic Microwave Integrated Circuit
<b>MoM</b>	Method of Moments
<b>MOSFET</b>	Metal Oxide Semiconductor Field effect Transistor
<b>MW</b>	Microwave
<b>NMSE</b>	Normalized Mean Square Error
<b>OFDM</b>	Orthogonal Frequency Division Multiplexing
<b>PAE</b>	Power Added Efficiency
<b>PAPR</b>	Peak-to-Average Power Ratio
<b>PA</b>	Power Amplifier
<b>PD</b>	Predistorter
<b>PCB</b>	Printed Circuit Board
<b>PSK</b>	Phase-shift Keying
<b>QAM</b>	Quadrature Amplitude Modulation
<b>RF</b>	Radio-Frequency
<b>RFC</b>	RF Choke
<b>RMS</b>	Root Mean Square
<b>SEM</b>	Spectrum Emission Mask
<b>SDR</b>	Software Defined Radio
<b>UMTS</b>	Universal Mobile Telecommunications System
<b>V2I</b>	Vehicle to Infrastructure



<b>V2V</b>	Vehicle to Vehicle
<b><math>V_{DS}</math></b>	Voltage Drain-Source
<b><math>V_{GS}</math></b>	Voltage Gate-Source
<b>VSA</b>	Vector Signal Analyzer
<b>VSG</b>	Vector Signal Generator
<b>WAVE</b>	Wireless Access in Vehicular Environments
<b>WLAN</b>	Wireless Local Area Network



# Chapter 1

## Introduction

### 1.1 Motivation

Radio communications have been evolving rapidly since its beginning until today. One can quickly understand the different reality between then and now just by analyzing the number radio systems used in daily activities, such as TV, FM Radio, Mobile Communications (like Global System for Mobile Communications (GSM), Universal Mobile Telecommunications System (UMTS) or Long Term Evolution (LTE)), Internet Access (Wi-Fi), Global Positioning System (GPS), etc. The inclusion of all these carriers in the same device influences the battery supply needed for devices like mobile phones. It is important to notice that the inclusion of all these technologies implies the use of high data transmission rates with mobile devices which need more efficient equipment to be able to work for a large time interval.

One part of these Radio Systems are the PAs, which are used in several fields and areas. As the name says, to amplify a signal, means that the output signal in terms of power should larger than the input signal. PAs are used for every communication system and so their characteristics are crucial for the successful implementation of a communication protocol. As it will be seen in the sections to come, efficiency and linearity are two important characteristics of a PA and they normally do not walk *hand in hand*.

In the particular case of this Dissertation, I am focused on the Microwave (MW) applications of such PAs. MW is a part of the Electromagnetic spectrum considered to be between, approximately, 1 GHz and 30 GHz (Figure 1.1), which is the electromagnetic

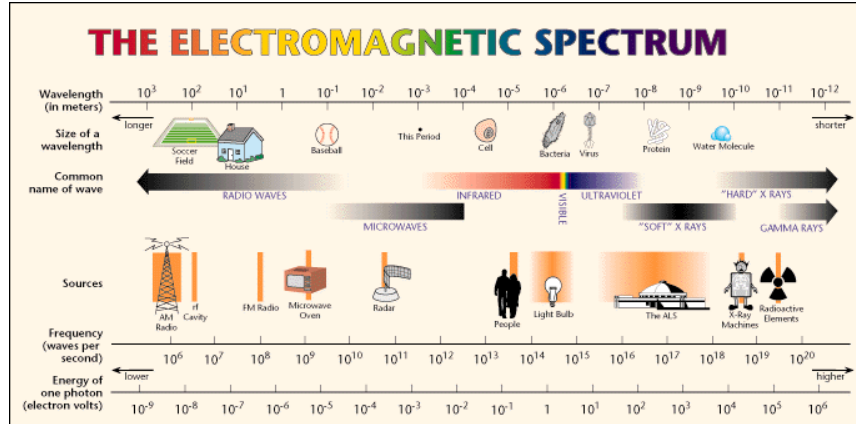


Figure 1.1: Electromagnetic Spectrum Distribution [1]

band used for cellular communications, Wireless Local Area Network (WLAN), WiMAX, GPS, among others. In the particular case of the work developed the goal was to design and implement the PA needed to fulfill the requirements of the IEEE 802.11p communication protocol. This protocol is used to add Wireless Access in Vehicular Environments (WAVE), supporting ITS applications. This way Vehicle to Vehicle (V2V) and Vehicle to Infrastructure (V2I) are allowed. Further considerations regarding IEEE 802.11p standard are described later on.

## 1.2 Objectives and Contributions

The objective of this thesis is to study the functioning and design of a Radio-Frequency (RF) PA suitable for wireless communications using the IEEE 802.11p standard at 5.9 GHz. Linearization techniques must be taken into account as well, either through Transistor Bias Point or DPD, in order to achieve the linearity necessary to fulfill the Spectrum Mask needed in this standard.

To accomplish this, the following points must be followed:

- Market analysis regarding transistor choice
- Design in Advanced Design System (ADS) of the Power Amplifier
- Study and implementation of DPD techniques
- Final testing and measurements

To disseminate this work, a paper entitled "*Design of a Power Amplifier for IEEE 802.11p applications*" was submitted to the conference *Eurocon 2015*, in Salamanca, Spain.

## 1.3 Structure

In the next paragraphs the structure of the document is explained, in order to understand the work done in this Dissertation.

In the first chapter the motivation, goals and structure of this Thesis are explained, regarding the components of each chapter.

In the second chapter Vehicular Communications as well as the IEEE 802.11p standard are described as this is the purpose of the PA designed. Besides this, other concepts such as Orthogonal Frequency Division Multiplexing (OFDM) are explained as they are integral part of the IEEE 802.11p standard.

In the third chapter a brief introduction about PA characteristics, such as Bias Point, Linearity, Efficiency, Technologies used in transistor manufacturing, etc, and knowledge needed to understand some approaches, such as S-Parameters.

During the fourth chapter the Design procedure is explained, from the selecting of the transistor and substrate to the use of ADS to improve certain results.

In the fifth chapter the results regarding the simulations are presented. These results show the performance of the PA in terms of one-tone and two-tone simulations as well as stability measurements.

In the sixth chapter, an introduction regarding DPD is done, as well as the explanation about the implementation of such algorithm, using memory polynomials.

Regarding the seventh chapter, the final measurements of the PA designed with and without DPD are done and discussed.

In the eighth and final chapter conclusions are discussed and future work is proposed.

# Chapter 2

## Framework

### 2.1 Vehicular Communications

Vehicular Communications are becoming more and more important in daily life, as everyone is looking for the self-driving car. In order to achieve this technology, vehicles must be able to communicate among them and also with the roadside units. In today's world, an example of a roadside unit is the tolls system *Via Verde* from Brisa, used in highways to allow costumers to pay the toll without stopping. The concept of vehicular communications would allow vehicles to share traffic, accident or weather information between each other and roadside units allowing safer roads. Another example is the possibility of leisure activities, such as Internet access, network games, chat, among others [2].

This is a concept that can allow telecommunications operators to provide new services to a niche market, specially regarding the leisure capacities of this network. In terms of the safety side of the equation, inter-vehicle communication is the future in terms of automobile and traffic management allowing the use of distributed networks over centralized networks, which have greater latency times, in a system where delay in the communications can be fatal, and require the use of sensors across the road making the implementation cost of such systems high [2].

Traffic management is one of the main interests of nowadays vehicular communications, since it is with this traffic management and communication between vehicles that self-driving cars can co-exist. As described in [3], traffic models are being created, using data like vehicular speed, density and flow, while trying to forecast the traffic for the next

15 to 20 minutes, allowing the drivers to plan alternative routes.

With the increased development of intelligent systems, the development and deployment of ITSs also moves forward, allowing V2V and V2I interactions to become more important and useful. From safety measures to traffic management control, vehicular communication systems are becoming more and more complex and will have increased importance in years to come.

### 2.1.1 IEEE 802.11p

This standard is similar to other 802.11x protocols, such as 802.11a or 802.11b, meaning that, as some versions of the other standards, it uses OFDM modulation which implies high Peak-to-Average Power Ratio (PAPR) [4]. In the case of LTE 4G the PAPR is normally between 8 to 12 dBm depending on the number of carriers used for the modulation. Since 802.11p also uses OFDM as a modulation technique it is possible to consider that the PAPR of such system can be close to the PAPR of an LTE system. Besides the OFDM another common characteristic for 802.11 standards is that the maximum output power of a PA is 1 Watt and the effective radiated power is 4 W [5]. The IEEE 802.11p was developed to allow WLAN in vehicular environments, being used in V2V and V2I communications.

The main differences of the protocol compared to 802.11a are listed below, considering information in [6]:

- **Bandwidth** In 802.11p, the 10MHz channels are usually used, in order to make the signal more robust against fading. The 20MHz are optionally implemented.
- **Carrier spacing** The 802.11p signal uses a carrier spacing reduced by  $\frac{1}{2}$  compared to 802.11a (due to the half clocked mode).
- **Symbol length** The symbol length is doubled making the signal more robust against fading (due to the half clocked mode).



- **Frequency** The 802.11p standard operates in the 5.9GHz frequency band, as the 802.11a operates in the 2.4GHz and 5GHz frequency bands.

Besides these differences, the ACPR as well as the SEM are more stringent in IEEE 802.11p than in IEEE 802.11a, especially in one of the power classifications created for this standard, Class D. This Class is the one that this design is trying to achieve.

Power Class	Expected Communication Distance (m)	Maximum Input Power of Antenna (dBm)	Maximum EIRP (dBm)
A	15	0	23
B	100	10	23
C	400	20	33
D	1000	28.8	33 for non Governmental
			44.8 for Governmental

Table 2.1: Maximum Transmitted Power for DSRC Band [6]

Power Class	Permitted power spectral density, dBc				
	+/- 4.5 MHz offset	+/- 5 MHz offset	+/- 5.5 MHz offset	+/- 10 MHz offset	+/- 15 MHz offset
A	0	$\pm 10$	$\pm 20$	$\pm 28$	$\pm 40$
B	0	$\pm 16$	$\pm 20$	$\pm 28$	$\pm 40$
C	0	$\pm 26$	$\pm 32$	$\pm 40$	$\pm 50$
D	0	$\pm 35$	$\pm 45$	$\pm 55$	$\pm 65$

Table 2.2: Transmitted Spectrum Mask for 10 MHz Channels [6]

As it can be observed in Tables 2.1 and 2.2, the class D constrictions are very demanding in terms of PA design, demanding a highly linear PA. As seen before, linearity presents an important factor when using a PA for a specific application such as IEEE 802.11p. Since linearities present one of the reasons for the increase width of the spectrum of a signal which leads to higher ACPR the SEM may not be fulfilled if the PA presents a high degree of non-linearities.

### 2.1.2 Orthogonal Frequency Division Multiplexing

Orthogonal Frequency Division Multiplexing (OFDM) modulation is widely used in communication systems such as wireless networks (IEEE 802.11a or Wi-Fi) or 4G (LTE) mobile communications since it allows a large number of closely spaced orthogonal sub-carrier signals to carry data on several parallel data streams/channels, dividing a bit stream into  $N_c$  substreams. This procedure leads to a distortion reduction of the overall signal. The basic principal behind OFDM is Frequency Division Multiple Access (FDMA). FDMA

requires the use of a guard band for each sub-carrier which results in a loss of efficiency as it can be seen in Figure 2.1.

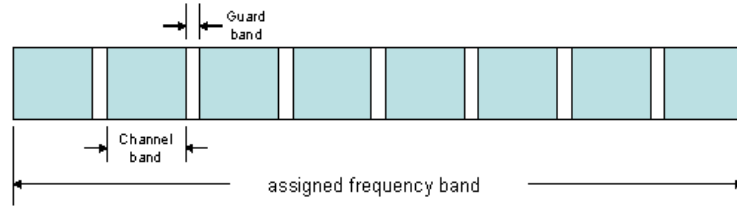


Figure 2.1: Example of the distribution of sub-carriers in FDMA and the guard band needed between them (Image taken from [7])

The main difference between FDMA and OFDM is that in the latter the carriers are orthogonal to each other (in frequency domain) which allows the elimination of the guard bands needed in FDMA[8]. This is easy to see with two sinc signals as in Figure 2.3. This way pulses can be transmitted at  $1/T$  rate within a  $1/(2T)$  bandwidth without Inter Symbol Interference (ISI), in case a Guard Interval is added. This Guard Interval contains the final samples of a bit stream and puts them in the beginning as shown in Figure 2.2.

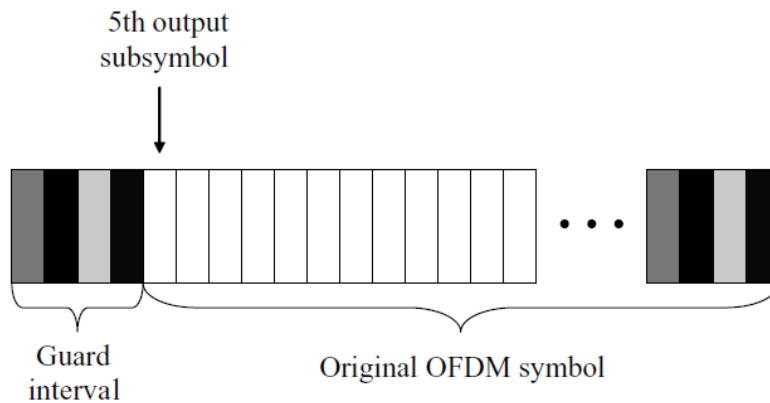


Figure 2.2: Use of Guard Interval to prevent ISI (Image taken from [9])

Each sub-carrier contains a commonly used modulation scheme such as Quadrature Amplitude Modulation (QAM) or Phase-shift Keying (PSK). A major drawback in terms of terrestrial use of OFDM is the high PAPR. This occurs because the independent phases of the sub-carriers can often combine constructively. The problem with PAPR is that it obliges the PA, to operate with a certain level of back-off, which in the case of LTE, for

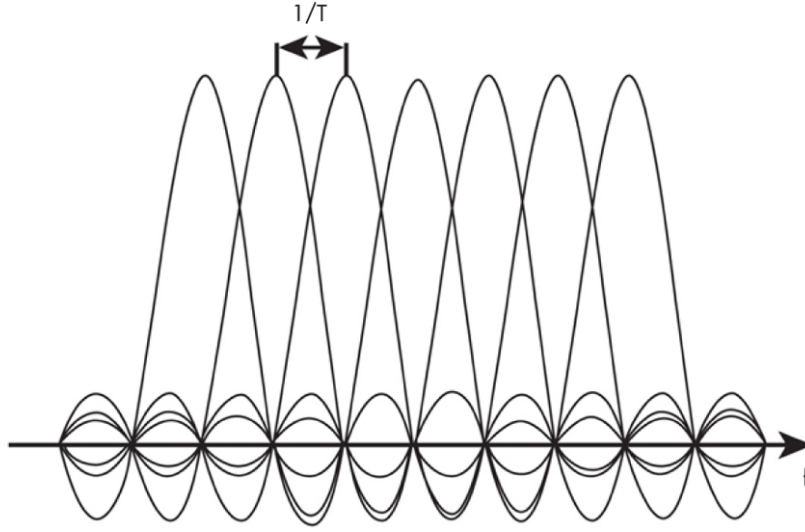


Figure 2.3: Sinc function representation in a OFDM application (Image taken from [10])

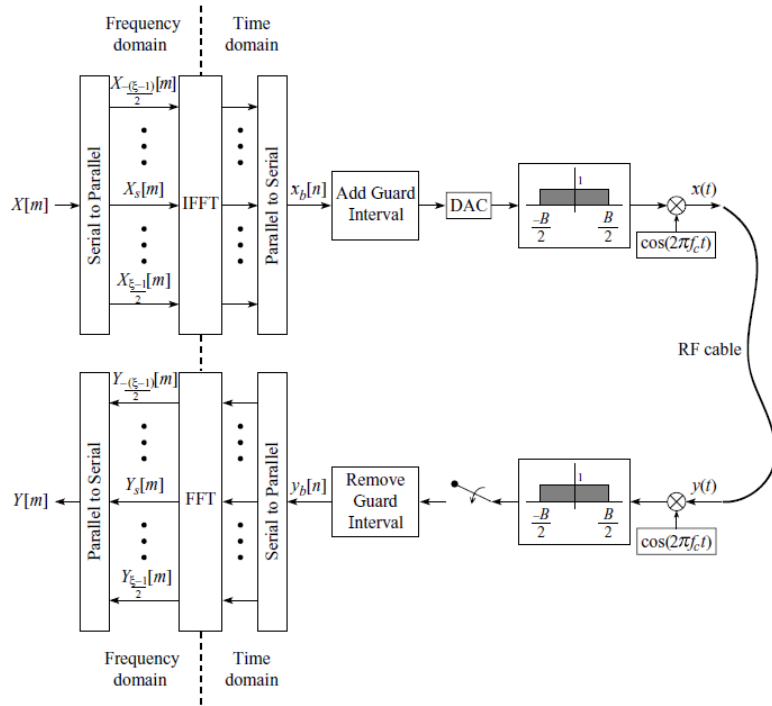


Figure 2.4: Representation of an OFDM system (Image taken from [9])

example, is about 8-12 dB, as stated in the beginning of this chapter. This means that efficiency will always be a problem in this type of systems/applications. This leads to one of the reasons of the design, where the main concern is the linearity rather than efficiency. Other problems related with OFDM concerning modulation are the complexity of the bank

of modulators, for example, but these problems are more concerned with the Digital part rather than the analog part so they are not approached in this Dissertation. Figure 2.4 shows a full OFDM system (apart from the RF front-end).

In short, the main advantages of OFDM are [11]:

- Good performance in selective fading channels
- Low-complexity of base-band receiver, requiring simple equalizers in frequency domain
- Good spectral properties
- Compatibility with multiple antenna technologies

The main drawbacks are [11]:

- Non-constant envelope of the modulated signal
- Reduced efficiency of the RF PA due to high PAPR

# Chapter 3

## Power Amplifiers

### 3.1 Introduction

One of the most important parts of a RF Front-end for communication systems is the PA. As a communication system, Vehicular Communications also need a PA. The development of this part of a Front-end allows the use of the RF part in Software Defined Radio (SDR) applications to improve the functionalities of V2V and V2I communications.

With this being said, this section presents a series of characteristics about PAs and also some adjacent knowledge needed to understand these characteristics.

### 3.2 S-Parameters

S-Parameters are used to describe the relationship between ports or terminals of a quadripole/two-port network. This two-port network can be anything: a resistor, a transmission line or an integrated circuit, for example, as long as it can deliver current or voltage.

S-Parameters are represented in a matrix called Scattering Matrix which is represented the following way [13]:

$$\begin{bmatrix} S \end{bmatrix} = \begin{bmatrix} S_{11} & S_{12} \\ S_{21} & S_{22} \end{bmatrix} \quad (3.1)$$

To better understand the Scattering Matrix it is important to know the definitions for each element of the Matrix, which can be seen from Eq. 3.2 to Eq. 3.5.

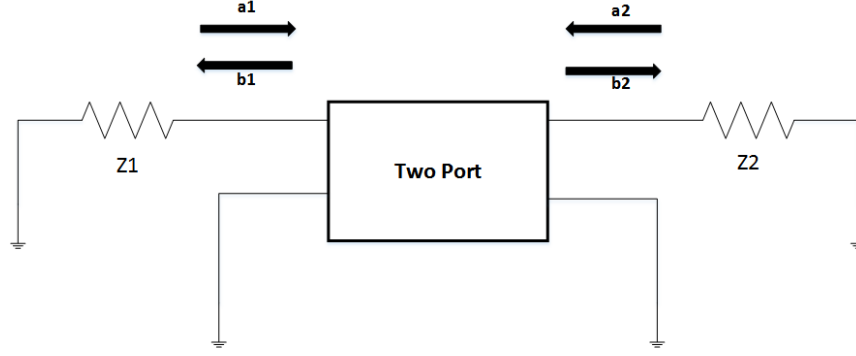


Figure 3.1: Representation of a two-port network (Image taken from [12])

---

$$S_{11} = \left. \frac{b_1}{a_1} \right|_{a_2=0} \quad (3.2)$$

*(input reflection coefficient with output properly terminated)*

$$S_{21} = \left. \frac{b_2}{a_1} \right|_{a_2=0} \quad (3.3)$$

*(forward transmission coefficient with output properly terminated)*

$$S_{22} = \left. \frac{b_2}{a_2} \right|_{a_1=0} \quad (3.4)$$

*(output reflection coefficient with input properly terminated)*

$$S_{12} = \left. \frac{b_1}{a_2} \right|_{a_1=0} \quad (3.5)$$

*(reverse transmission coefficient with input properly terminated)*

Where,  $a_i$  and  $b_i$  present the coefficients given by equations 3.6 and 3.7 [14]:

$$a_i = \frac{V_i + Z_i I_i}{2\sqrt{\text{Re}Z_i}} \quad (3.6)$$

$$b_i = \frac{V_i - Z_i^* I_i}{2\sqrt{\text{Re}Z_i}} \quad (3.7)$$

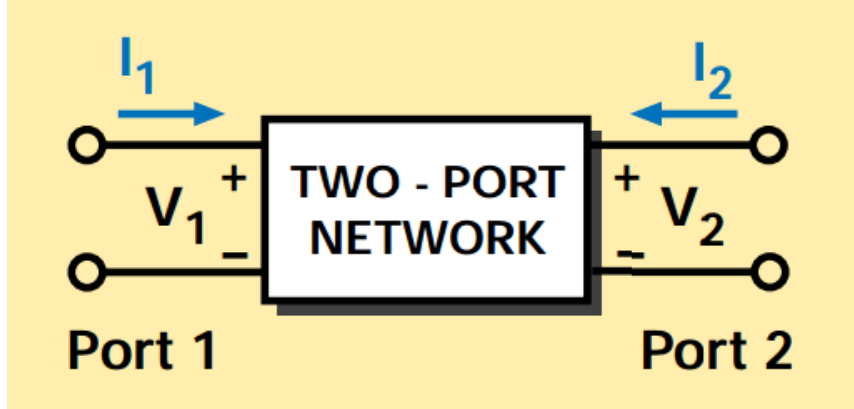


Figure 3.2: Representation of a two-port network using Voltages and Currents(Image taken from [14])

$V_i$  and  $I_i$  are the voltages and currents at the ports of the two-port network as represented in Figure 3.2.

When using a two-port network in a transistor, the transistor has to be properly biased. Another important factor is that the S-Parameters of a transistor must be measured under small-signal conditions. As important as this, is the fact that the S-Parameters of a transistor change with the frequency.

Using S-Parameters presents a great advantage that comes from its definition: they are measured using a matched termination[13]. Consider this a very brief explanation of S-Parameters but the enough for the scope of this Thesis.

### 3.3 Bias Point and Classes of Operation

Within PAs, the traditional classes of operation are A, AB, B, C, where the transistor works as a controlled current source, which then lead to different classes of operation such as D, E or F that are derivations of the traditional ones, where the transistor works as switching device. These differ in terms of conduction angle, efficiency, linearity and gain. The class selection is made through the setting of the Bias point for the transistor for classes A, AB, B and C. The Bias Point and the Drain-Source DC current ( $I_{DC}$ ) are related. Considering Class A as a first example, lets evaluate Figure 3.3.

As it can be seen in Figure 3.3, a Class A amplifier is characterized by the fact that it

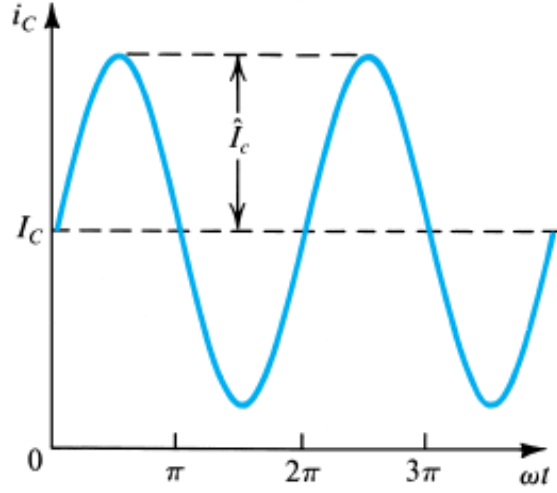


Figure 3.3: Class A conduction angle (Image taken from [15])

conducts for the entire cycle of the input signal [15], which means the conduction angle is 360 degrees. Class A acts as a current source controlled by the gate drive and bias point [16].

In terms of conduction angle the next step is Class B (Figure 3.4) which means a conduction angle of 180 degrees, thus meaning that the transistor, when having a sinusoid input, only conducts during the positive slope of that same sinusoid. This happens due to the fact that a Class B PA is biased using zero DC current. It is easy to see that this lack of conduction angle will lead to non-linearities, which will be discussed later.

This leads us to the next class of operation: Class AB. As the name states it works between Class A and Class B, thus meaning that the conduction angle is between 180 and 360 degrees (Figure 3.5), accomplished because the biasing of the transistor is done with a nonzero DC current much smaller than the peak current [15].

Apart from these 3 types, other types exist, among them Class C, which is when the transistor conducts for an angle smaller than 180 degrees (Figure 3.6). Other examples, such as Class F are derivations of the 4 main classes described above as said before. Class F can be used to increase the efficiency of a design made in class AB or B. To understand the following procedure it is important to notice that in RF PA design the harmonics of a signal are normally treated in a certain way to improve the efficiency of the overall system. In classes AB and B the harmonics of the signal are short circuited whereas in class F the



odd harmonics are open circuited and the even harmonics are short circuited. This leads to approximately square waves of voltage and half-sine wave for current (Figure 3.7)). If infinite harmonics could be done, a perfect square wave and a perfect half-sine wave is achieved [17] and 100% efficiency is obtained. In practical terms only the 2<sup>nd</sup> and 3<sup>rd</sup> harmonics are considered due to high frequency losses in materials which leads to a maximum of over 80% efficiency in class F amplifiers. Due to this fact, class F PAs are becoming more common when designing for highly linear configurations.

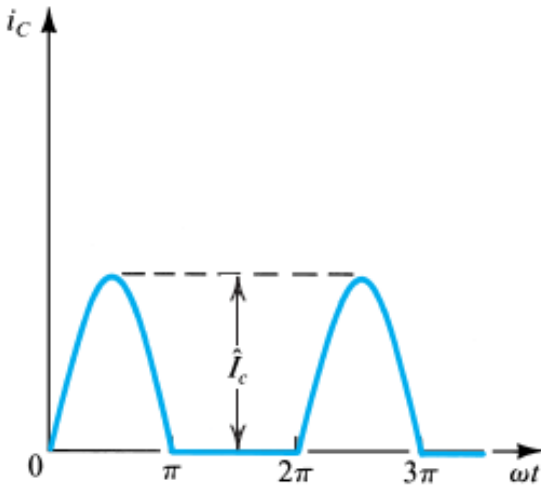


Figure 3.4: Class B conduction angle (Image taken from [15])

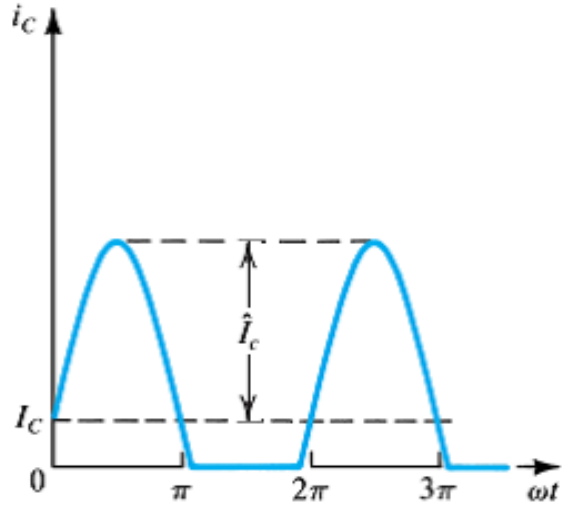


Figure 3.5: Class AB conduction angle (Image taken from [15])

Besides the conduction angle, other characteristics vary according to the Bias Point of the transistor, such as gain, efficiency and output power, as said before. To better understand the values related to each class of operation, first it is important to understand how to calculate the max output power and the efficiency of the transistor.

The max power given to a certain load by a transistor takes into consideration the conduction angle of such transistor (and therefore its bias point).

$$P_{L_{max}}(\theta) = \frac{1}{4\pi} \cdot V_{DC} \cdot I_{max} \cdot \frac{2\theta - \sin(2\theta)}{1 - \cos(\theta)} \quad (3.8)$$

In equation 3.8,  $V_{DC}$  represents the voltage supplied by the voltage supply and  $I_{max}$  the maximum current in the transistor.

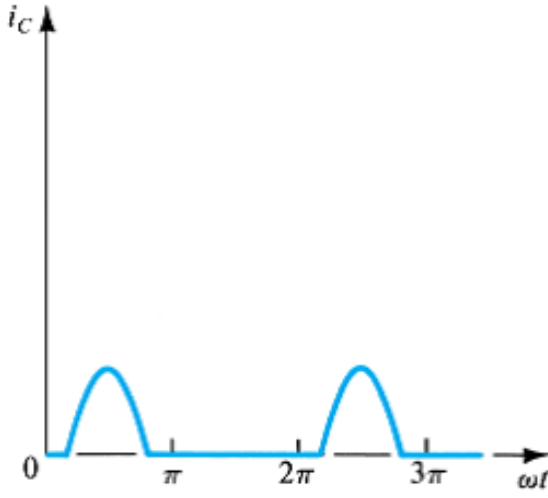


Figure 3.6: Class C conduction angle (Image taken from [15])

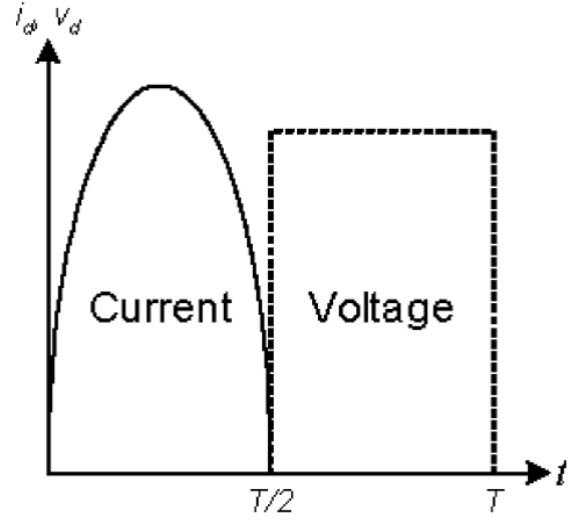


Figure 3.7: Class F conduction angle (Image taken from [17])

The efficiency of the amplifier is dependent from the max output power and the DC power supplied to the transistor. This means that, intrinsically, it also depends on the conduction angle of the transistor.

$$\eta_{max} = \frac{P_{L_{max}}}{P_{DC}} = \frac{1}{4} \cdot \frac{2\theta - \sin(2\theta)}{\sin(\theta) - \theta \cos(\theta)} \quad (3.9)$$

To better understand the differences between classes A, AB, B and C Table 3.1 summarizes the values expected for each case.

Operation Class	Conduction Angle ( $2\theta$ )	Maximum Output Power	Maximum Efficiency
A	$360^\circ$	$\frac{1}{8} \cdot V_{DC} \cdot I_{max}$	50%
AB	$180^\circ < 2\theta < 360^\circ$	$P_{L_{Max}}(\theta)$	$78.5\% < \eta_{Max} < 50\%$
B	$180^\circ$	$\frac{1}{8} \cdot V_{DC} \cdot I_{max}$	78.5%
C	$0^\circ < 2\theta < 180^\circ$	$P_{L_{Max}}(\theta)$	$100\% < \eta_{Max} < 78.5\%$

Table 3.1: Characteristics of each Bias point using conduction angle. [18]

## 3.4 Linearity

### 3.4.1 Linear and Non-Linear Systems

Before approaching Linearity in PAs it is important to understand the linearity concept from a mathematical perspective.

Linearity is a concept that incorporates both proportionality and superposition principles. This means if  $x(t)$  is an input signal to  $y(t)$ , then the sum of the responses of  $y_1(t)$  and  $y_2(t)$  to  $x_1(t)$  and  $x_2(t)$ , respectively, must be equal to the response of  $y(t)$  to the sum of  $x_1(t)$  and  $x_2(t)$ . The next mathematical equations help understand this situation.

$$y_1(t) = a_1 \times x_1(t) \quad (3.10)$$

$$y_2(t) = a_1 \times x_2(t) \quad (3.11)$$

$$y(t) = y_1(t) + y_2(t) \quad (3.12)$$

These systems are much easier to understand than non-linear systems. Nevertheless most of real systems are non-linear, whose mathematical approaches involve more calculations and processing than linear systems. However, due to mathematical tools available nowadays, some non-linear systems can be, under certain conditions, treated as linear-systems.[19]

Besides all this, and before moving on with Linearity in PAs, it is good to know that other systems use non-linearities in a positive way. For example, mixers or frequency multipliers, could not exist if there were no non-linearities [19].

### 3.4.2 Linearity in Power Amplifiers

Regarding linearity in PAs, there are two ways to understand it, either through gain (AM-AM characteristic) or the signal phase related to the input signal (AM-PM characteristic). If both AM-AM and AM-PM represent a constant relation in the PA for a certain region of operation, then the PA is linear in that region. These curves can be found in Figure 3.8.

To achieve the linearity there are two options considering only the bias point: either Class A is selected (which is the most linear class of operation) or a transistor is used in

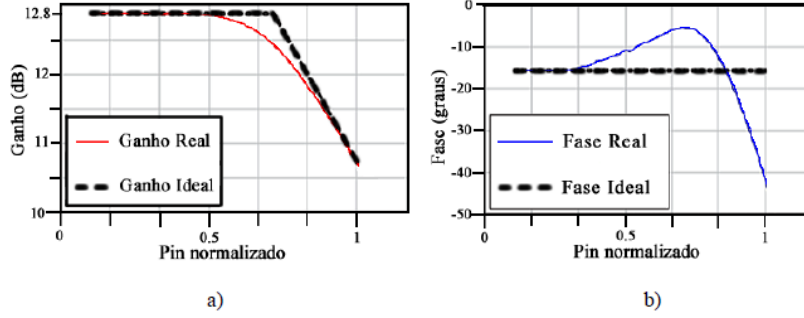


Figure 3.8: AM-AM (a) and AM-PM (b) real and ideal curves (Image taken from [18])

back-off mode while biased in Class AB/B. The back-off mode means that, i.e., a transistor is able to provide 40 dBm of Power output at 1dB compression point, for example, and only 28 dBm will be used. The non-linearities introduced by amplification of the signal decrease the quality of the SEM which is an extremely important factor when designing PAs to obey a certain communication protocol as the WLAN case. This is even further noticed when considering the cases of Power Classes C and D of IEEE 802.11p where the SEM is very stringent.

Another way of improving linearity is the use of a DPD. A DPD is used in cases where linearity is needed but efficiency is also important. This means that a DPD helps maintain the Output/Input ratio (gain) as well as the phase angle between the input and output signal. These effects originate in-band and out-of-band distortion which compromises the SEM and consequently the overall quality of the system. In the scope of this thesis, efficiency is not the main goal but linearity is. Nevertheless, using Class AB or B improves the Output Power of the transistor which helps achieving the back-off needed due to the high PAPR value.

### 3.5 1dB Compression Point

The 1dB Compression Point is correlated to the Linearity of a PA and it is normally considered regarding the ideal behavior of a PA. This means that the 1dB Compression Point is the operation point where the real Gain curve (or AM-AM characteristic) is 1dB below the ideal Gain curve. This means that 2dB Compression Point or 3 dB Compression Point can also be considered depending on the situation. As the gain compresses more and more, the non-linearities of the PA also increase.

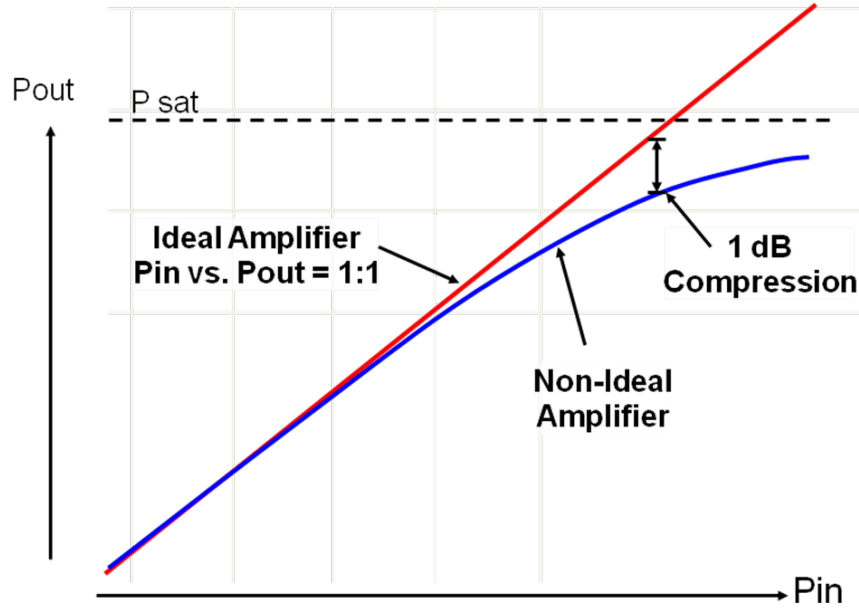


Figure 3.9: Power output versus Input Power in a generic Power Amplifier with 1dB Compression Point Illustration (Image taken from [20])

### 3.6 3rd Order Interception point

The Third order Interception Point (IP3) is another way of characterizing the linearity of a PA. This way of evaluating the linearity of a circuit has an advantage since the distortion caused by the circuit can be computed for any input power level, as it can be seen in Equation 3.13, where  $G$  represents the Gain of the PA,  $P_{in}$  the input power of the PA and  $P_{IMD}$  the distortion power. Figure 3.10 showcases how the IP3 can be obtained.

$$IP3(dB) = \frac{3(G + P_{in}) - P_{IMD}}{2} \quad (3.13)$$

### 3.7 Efficiency

The linearity problem leads to another important feature in PAs: efficiency. Since there are many portable devices nowadays used in, for example, cellular communications, having a low-efficiency PA is not desirable. Regarding this situation, using a Class C PA would be a good decision. However due to the non-linearities of such bias point, this is not always a good solution, so Class AB/B is a better option. Nevertheless, using Class C for linear systems can be an option if the PA is used with a DPD which compensates

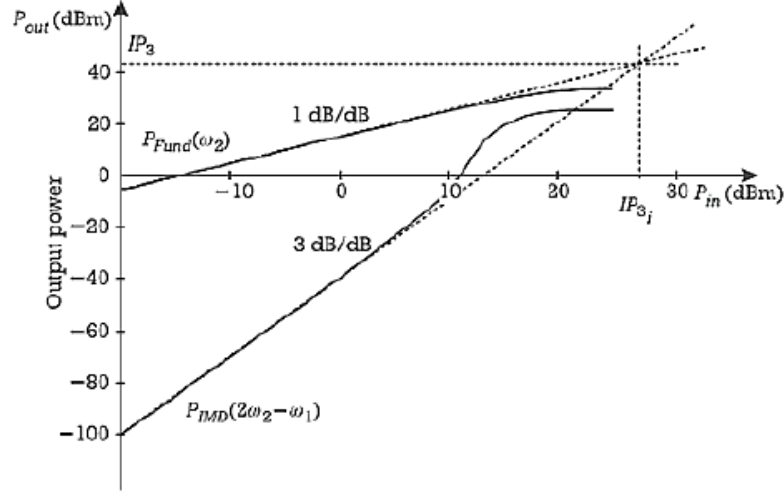


Figure 3.10: Representation of the 3rd Order Interception Point (Image taken from [21])

the non-linearities in the PA, as described before. Nevertheless it is important to consider that the more non-linear an amplifier is, the more complex a DPD will be, which in some cases can request higher computational power and so higher power consumption as well.

### 3.7.1 Power Added Efficiency

PAE is a way of measuring the efficiency of a PA which is a bit different from the traditional efficiency  $\eta$ , presented in Equation 3.9. Where as  $\eta$  only presents a ratio between the RF power delivered to the load and the DC power, PAE presents a definition between the output power and the input power divided by the DC power as it can be seen in Equation 3.14.

$$PAE = \frac{P_a}{P_{DC}} = \frac{P_{out} - P_{in}}{P_{DC}} \quad (3.14)$$

PAE is important since, when the output power increases significantly, "the gain loses importance as a valuable performance evaluation tool" [21], thus giving origin to the ratio between added power and supply power as seen in Equation 3.14. As it will be seen later in the simulations and result presentations, the PAE is one of the PA characteristics taken into account when evaluating its performance.

### 3.8 Adjacent Channel Power Ratio (ACPR)

ACPR (also known as adjacent channel leakage ratio) is related to the effect of non-linearities in adjacent channels. It is a measurement done nowadays since it allows the user to evaluate the distortion caused by the amplifier in the adjacent channels. It is "the ratio of the power in a specified band outside the signal bandwidth to the Root Mean Square (RMS) power in the signal" [22]. Figure 3.11 illustrates better this situation.

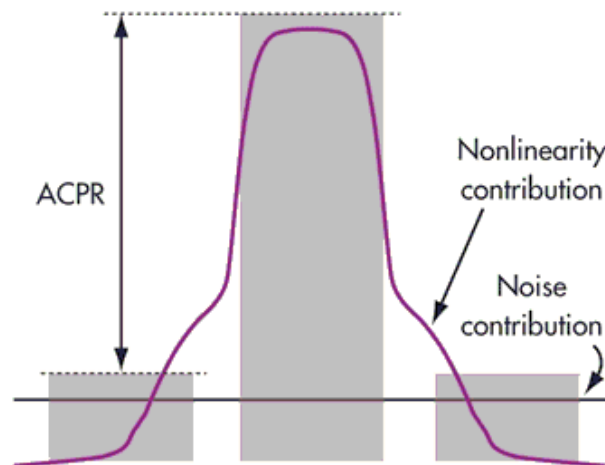


Figure 3.11: Representation of the ACPR effect due to non-linearities (Image taken from [23])

### 3.9 Stability

Stability is another important aspect when designing a PA. "The fundamental definition of a stable electrical network is that its response is bounded when the excitation is bounded" [19]. When relating this to a linear two-port network, it means that the poles of the network must be on the left half of the complex plane. An unconditionally stable amplifier is what designers try to achieve in a large bandwidth. Stability issues can occur at low-frequencies (for example, sub-harmonics), the frequency of operation or at  $n$ -th order harmonics. This means that for each case there are different ways to prevent instability issues in the PA. The K-factor, also known as the Rollet Stability Factor, is a way of understanding if a PA can be stable or not. The K-factor takes into consideration the S-Parameters of a transistor and it is given by equation 3.15.

$$K = \frac{1 - |S_{11}|^2 - |S_{22}|^2 + |\Delta|^2}{2|S_{12}||S_{21}|} \quad (3.15)$$

Where,

$$\Delta = S_{11}S_{22} - S_{12}S_{21} \quad (3.16)$$

In practical terms it can be said that if  $K > 1$  and  $|\Delta| < 1$ , the two-port network is unconditionally stable. However, and as presented by [24], if instead of Equation 3.16 being less than 1, Equations 3.17 or 3.18 are greater than zero, stability is also achieved.

$$B_1 = 1 + |S_{11}|^2 - |S_{22}|^2 - |\Delta|^2 \quad (3.17)$$

$$B_2 = 1 + |S_{22}|^2 - |S_{11}|^2 - |\Delta|^2 \quad (3.18)$$

Another way of understanding stability and measuring it are the  $\mu_{source}$  and  $\mu_{load}$  coefficients. These coefficients can be used in the same way as the  $K$  and  $\Delta$  to study the stability of a two-port network.

$$\mu_{source} = \frac{1 - |S_{11}|^2}{|S_{22} - \Delta(S_{11}^*)| + |S_{21}S_{12}|} \quad (3.19)$$

$$\mu_{load} = \frac{1 - |S_{22}|^2}{|S_{11} - \Delta(S_{22}^*)| + |S_{21}S_{12}|} \quad (3.20)$$

If both  $\mu_{source}$  and  $\mu_{load}$  are greater than 1, then the two-port network is unconditionally stable [24]. Both of these geometric stability coefficients are used in ADS simulation and thus are important for the analysis of the stability of the PA designed. As it can be seen, it is easier to use geometric stability coefficients since there are less equations to be calculated to investigate about the stability of a certain circuit.

These pre-requisites can be obtained with different techniques and the one used in this design will be discussed later on in Chapter 4.



## 3.10 Technologies

RF PAs use different active devices which include, Bipolar Junction Transistors (BJTs), Metal Oxide Semiconductor Field effect Transistors (MOSFETs), Junction Gate Field effect Transistors (JFETs), Gallium Arsenide Field effect Transistors (GaAsFETs), Metal Semiconductor Field effect Transistors (MESFETs), High electron mobility Transistors (HEMTs), among others. Depending on the technology used and the purpose of the PA, the output power varies as well as the range of frequency operation. These characteristics also take into account the packaging of the transistor, which can be on chip, Monolithic Microwave Integrated Circuit (MMIC), etc. Another important point is that most transistors operate in an n-p-n junction "because the greater mobility of electrons (versus holes) results in better operation at higher frequencies"[16]. This is an important factor since nowadays developments in the K-Band/Infrared (about 20 to 40 GHz as seen in Figure 1.1) are more and more common and looks like communications in this high frequency can have a great impact in future work and technology development.

Regarding the Gallium Nitride (GaN) HEMT transistors, they have higher output power capabilities than most GaAsFET, in terms of MW PAs, being capable of operating at high temperatures. This means that they can operate with less protections, reduced size cooling systems and an increase in longevity in adverse environments. Having a higher power density also allows the design of smaller power modules when compared to the ones that use GaAsFET transistors [25].

As a curiosity for technology development in transistors, Figure 3.12 shows the cutoff frequencies for the transistors produced with different technologies.

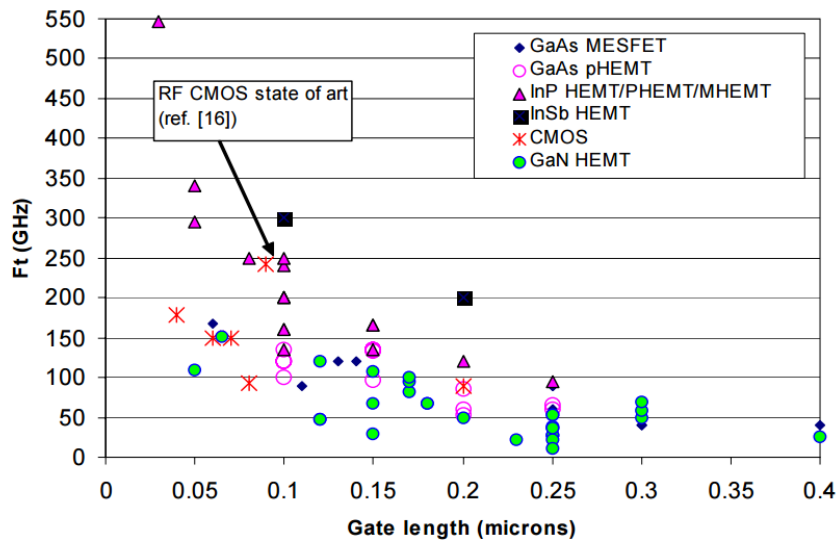


Figure 3.12: Transistor cut-off frequency comparison for various device technologies - data from 2005 (Image taken from [25])

# Chapter 4

## Power Amplifier Design

In this chapter the design procedure is described. To better understand the steps needed, the following sections are presented:

- Transistor and Substrate
- Bias Point
- Load-Pull
- Source-Pull
- Bias Network
- Impedance Matching Networks and Stability
- Minor Adjustments and Optimizations

The Design simulations and procedures were done using Advanced Design System (ADS) from Keysight Technologies.

### 4.1 Transistor and Substrate

The first step in the Design is to choose a transistor that is available on the market and can fulfill the requirements needed for its use. First, the transistor chosen should work in the 5.9 GHz region, due to the IEEE 802.11p standard. Besides this, and because the goal is to achieve Class D communications, the output power of the PA should be at least 28.8 dBm plus an added value of PAPR which is considered to be about 10 dB for this design,

considering the specifications of LTE standard.

With this in mind, and rounding the values of output power, the transistor should be able to provide to the load at 1 or 2dB compression point (more on this later), about 40 dBm of Power. To achieve this, the transistor chosen is the CREE CGH55015 suited for this type of applications. The complete datasheet of this device can be found in [26].

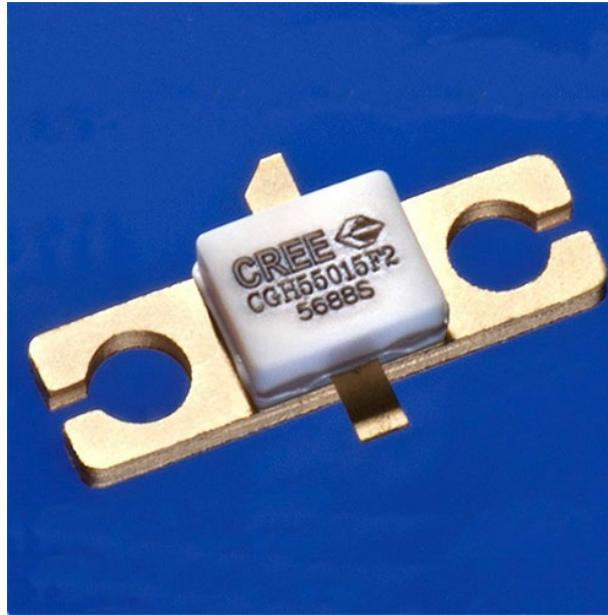


Figure 4.1: CREE CGH55015 transistor (Image taken from [27])

Moving on from the transistor, the substrate is another important factor in the design of a RF PA. A substrate should have a consistent  $\epsilon_r$  over the whole board and adding to that it is convenient that the Tangent Loss value is also as low as possible. Considering this and the substrates available at our facilities, it was decided that the Substrate should be 4350B from Rogers. The most important specifications of the device can be found in Table 4.1.

## 4.2 Bias Point

In order to select the Bias Point, linearity and efficiency are two important factors for this choice. Considering this and relating it to the IEEE 802.11p standard requirements, biasing the transistor in Class AB mode can be a good decision. Class AB as described

Parameters	Value
Substrate Thickness	0.762 mm
Conductor Thickness	35 $\mu\text{m}$
Dielectric Loss Tangent	0.0031
Relative Dielectric Constant	3.66

Table 4.1: Rogers 4350B substrate characteristics

before consists in biasing the transistor with a very small drain current compared to maximum DC current possible. Apart from this, the manufacturer suggests the value of 28 V for Voltage Drain-Source ( $V_{DS}$ ).

To measure this, the setup presented in 4.2 was used in ADS.

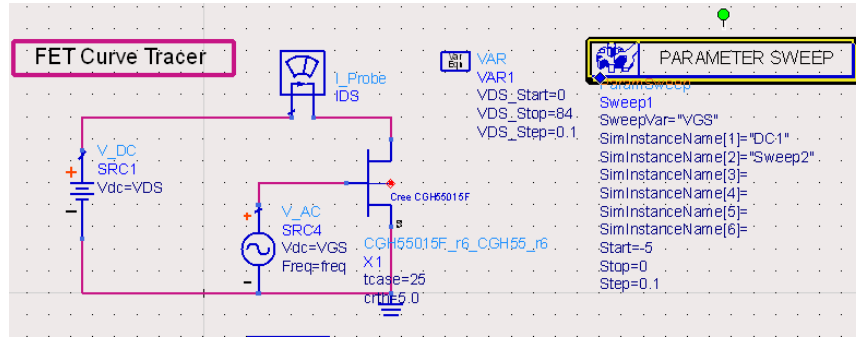


Figure 4.2: Setup to get I-V Curves of the transistor

As it can be seen in Figure 4.3, the Voltage Gate-Source ( $V_{GS}$ ) selected is -2.9 V and the  $I_{DS}$  is 110 mA, about 5% of the maximum  $I_{DS}$  current, which is about 2 A.

### 4.3 Load-Pull

After deciding on the Bias Point of the transistor, the next step is to do a Load-pull characterization to know which is the best load that the transistor should *see* in order to fulfill our goals. When doing Load-pull, Efficiency and Output Power curves are obtained and presented in a Smith Chart. Normally the maximum of output power point does not correspond to the maximum efficiency point so this means that the designer must choose what is more important or make a compromise between the two.

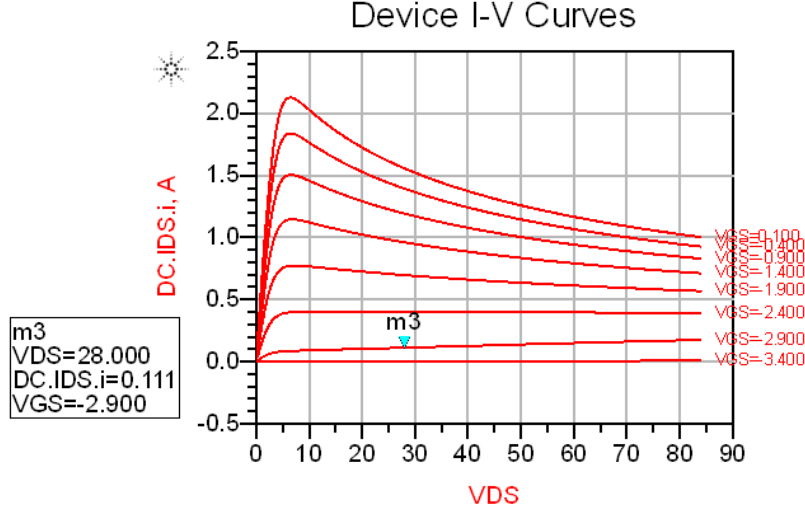


Figure 4.3: Choice of Bias Point for the PA

In the particular case of this design, since Efficiency is not something we are very concerned due to the particular application of the PA, achieving the maximum Output Power is the goal. In the particular case of this Thesis the goal is to be able to achieve about 40 dBm of output power at 1 or 2dB compression point so that the high PAPR of the standard can have a smaller influence in the non-linearities of the device. With this being said Figures 4.4 and 4.5 present both the setup used to get the load-pull for this transistor and the results. In the setup used the number of points and area of the Smith Chart to be tested can be chosen, which means that after a first general test, it was decided that the best load could be achieved in the area shown in Figure 4.5.

One important aspect in this setup is the impedance of the load in the harmonic frequencies. Due to constraints in the constructions of the Printed Circuit Board (PCB) the only harmonic taken into consideration is the second harmonic which goal is to short-circuit. Short-circuiting the harmonics of a signal is one of the characteristics of a Class B amplifier[28].

When doing the Load-pull it is important to understand that the Source Impedances on Terminal 1 (view Figure 4.4) also have influence in the results presented by this simulation. Considering this factor, the source impedance at 5.9 GHz used in this simulation is the one presented by the manufacturer at 5.8 GHz and, as in the load impedances, the

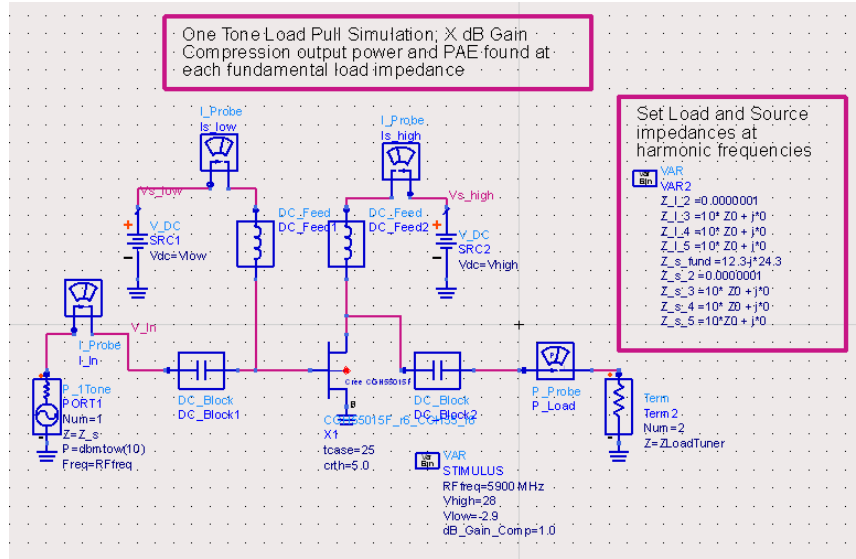


Figure 4.4: Load-Pull setup

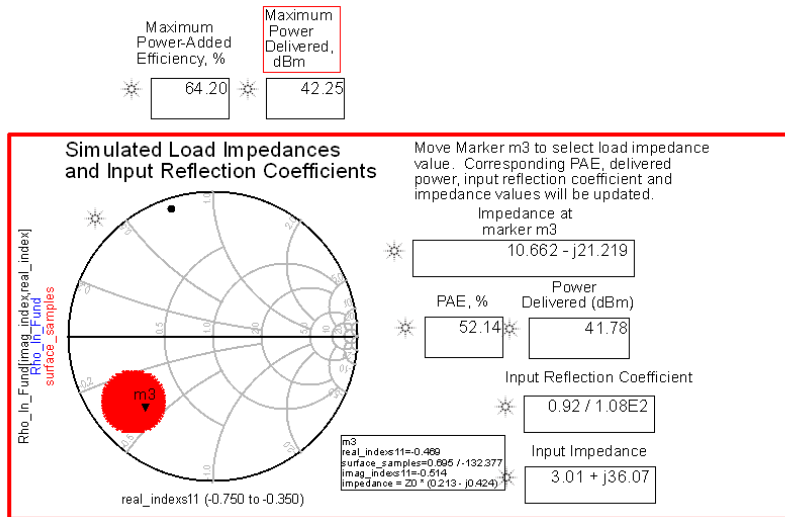


Figure 4.5: Load-Pull results

2<sup>nd</sup> harmonic is short-circuited as well, for the same reason.

## 4.4 Source-Pull

Since in the case of the application of this transistor we are more worried about Power Output and gain, Source-Pull characterization was not done. Instead, after obtaining

the Load Impedance from the Load-Pull simulation, the impedance *seen* at the Gate of transistor was registered and then, to achieve the maximum Power delivered the Source Impedance used was the complex conjugate of the Gate Impedance [29].

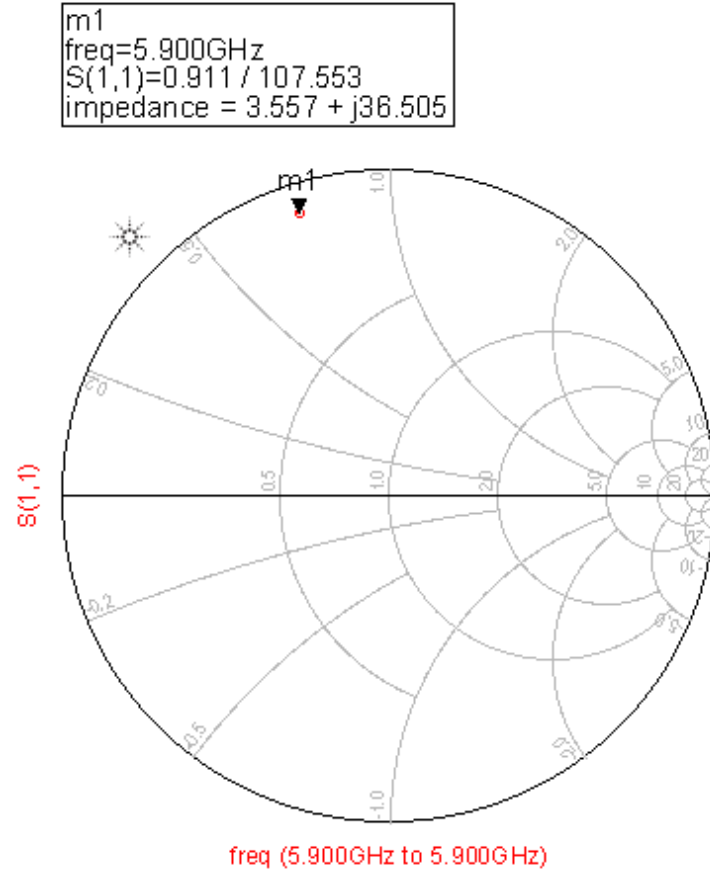


Figure 4.6: Source Impedance seen at the gate of the transistor

As said before the complex conjugate impedance is the one used in this case so the desired impedance of the Impedance Matching Network (IMN) is  $3.557 - j36.505 \, \Omega$ . It is important to notice at this point, that when doing the IMN, the Impedance achieved with those networks will not be exactly the same as the one obtained in the Load-Pull calculations. Due to this reason, the Source Impedance evaluation will be repeated after the design of the Output IMN to review this value.



## 4.5 Bias Network

To do the Bias Network it is important to consider the importance of such part in the design of a PA. Designing a good Bias Network implies that the proper bias point will be held over variations in transistor parameters and temperature [13]. Adding to this, no signal should be *lost* in the Bias Network. This means that at the frequency of operation, the signal should face an open circuit impedance in the path of the Bias network. To achieve this the proper method of doing this is called RF Choke (RFC).

So, how to achieve this open circuit impedance? The easiest way when considering RF applications is to do it with a  $\frac{\lambda}{4}$  transmission line. What this transmission line does is basically invert the impedance seen on the other point of the circuit as it can be easily illustrated with a Smith Chart as in Figure 4.7. If we start from the left end of the Smith Chart, with an impedance of Zero  $\Omega$ , and use a  $\frac{\lambda}{4}$  rotation (half of the Smith Chart), then the impedance shifts to the right end of the Smith Chart which is equal to an infinite impedance, also known as a open-circuit, which the impedance the bias network tries to achieve, relative to the signal at the frequency of operation.

This can also be explained using the Input Impedance of a lossless transmission line, as shown in Equation 4.1.

$$Z_{in}(l) = Z_0 \frac{Z_L + jZ_0 \tan \beta l}{Z_0 + jZ_L \tan \beta l} \quad (4.1)$$

If  $Z_L$  is the load impedance and  $Z_0$  the characteristic impedance of the line, and at the load of the line it is used a short circuit the expression can be simplified to:

$$Z_{in}(l) = Z_0 j \tan \beta l \quad (4.2)$$

From this simplification, equations 4.3 show the steps to achieve the final result.

$$Z_{in}(l) = \infty \quad (4.3a)$$

$$\infty = Z_0 j \tan \beta l \quad (4.3b)$$

$$\tan^{-1} \infty = \beta l \quad (4.3c)$$

$$\text{If, } \beta = \frac{2\pi}{\lambda}, \text{ then} \quad (4.3d)$$

$$\frac{\pi}{2} = \frac{2\pi l}{\lambda} \quad (4.3e)$$

$$l = \frac{\lambda}{4} \quad (4.3f)$$

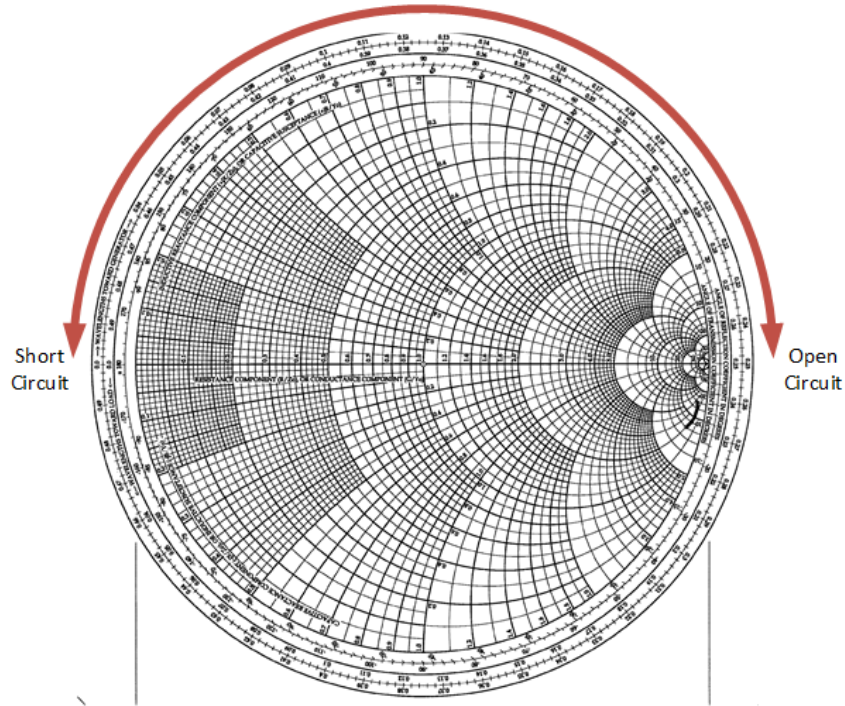


Figure 4.7: Example of the transformation of a short-circuit to an open-circuit using a  $\frac{\lambda}{4}$  transmission line.

If a short circuit at the frequency of operation is needed at that point of the transistor, then the correct way to do it is to add a Capacitor that has a very low impedance at the frequency of operation desired. Combining this with a radial stub, to increase bandwidth of this operation, our Bias Network is almost completed. This procedure is explained as well in Figure 4.7. The only thing missing is 3 other Capacitors that have an increase in

their value in about 100 times for each capacitor. They are used due to the DC Voltage source ripple and possible instabilities at very low frequencies. As a safety measure, and as suggested by the manufacturer, in the Bias Network of the Gate, a resistor of about 22 or 50  $\Omega$  should be used, regarding stability issues at low-frequencies. In the case of this design, a resistor of 50 $\Omega$  was used. This 50 $\Omega$  resistor is only used in the Bias Network at the gate of the transistor, as it can be seen comparing Figures 4.8 and 4.9.

Figure 4.8: Input Bias Network

In order to do the Bias Networks presented in Figures 4.8 and 4.9, optimizations techniques from ADS were used. These techniques simplify the design process, since it allows the user to give a certain goal to the design along with limitation for the values of the components (in this case the transmission line and the radial stub). This way the results are achieved more efficiently with less effort. This technique will be used for all IMNs.



## 4.6 Impedance Matching Networks and Stability

After designing the Bias Network the next step is to design the IMN and consider stability conditions. IMNs are important since they can convert a certain impedance value to another. In practice, and translating to the specific case of this Thesis, when the Load-Pull was done a certain load was obtained for which the transistor had a good response. The problem is that that impedance is not equal to  $50\ \Omega$ , which is the conventional impedance when feeding signal to a transistor or when connecting it to an antenna or Vector Signal Analyzer (VSA), for example. Apart from this, a DC Block capacitor must be used to avoid DC current to go to the load. This Capacitor should also be close to a Short-Circuit at the frequency of operation. In this section, the Output IMN is done first place, then stability conditions are evaluated and then the Input IMN is done.

### 4.6.1 Capacitors

After using the S-Parameter Models from ATC800A series to measure the impedance of the transistors at the 5.9 GHz frequency the 1pF Capacitor was the one chosen. It was also seen by the software provided by ATC, Tech Select, that this capacitor has Series Resonance of about 10 GHz which is above the frequency of operation thus making it valid for this implementation. Another possibility can be the 3.3 pF capacitor which has a series resonance of about 7.1 GHz. Even though with the S-Parameter model the 1 pF seemed to have a better performance, when building the circuit this change may be needed due to manufacturing problems. The impedance at 5.9 GHz presented by the capacitor from the S-Parameter model can be seen in Figure 4.10

### 4.6.2 Output IMN

Regarding the Output IMN and the Load-Pull data, the impedance to be converted to  $50\ \Omega$  was  $11.009 - j*16.946\ \Omega$ . To be able to do this transformation 3 open-circuit stubs were used, since besides doing the transformation at the frequency of operation, short-circuiting the 2<sup>nd</sup> harmonic was also a goal. Besides this, and to finish with a  $50\ \Omega$  line a Taper was used to decrease the width of the last transmission line gradually. After defining the minimum and maximum values wanted for width and length of the transmission lines, a optimization algorithm in ADS was used to perform this adaptation. The width

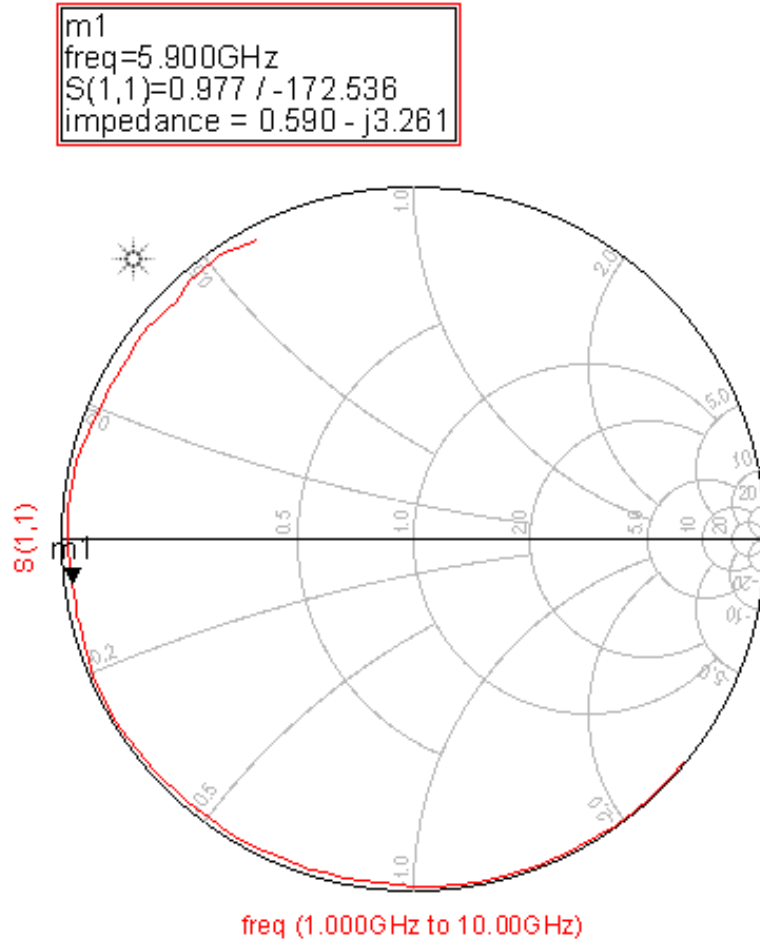


Figure 4.10: Impedance of the capacitor between 1 and 10 Ghz

minimum and maximum values were defined taking into account the impedances of about  $100\Omega$  and  $10\Omega$ , respectively. In terms of length, the minimum length was about 3 mm and the maximum length was inferior to  $\frac{\lambda}{2}$ . That minimum was selected to force the IMN to have a line-stub appearance to help guarantee that in reality it behaves in close manner to the schematic simulation.

As said before the design of this IMN is done using optimization techniques from ADS after defining the limits for the width and length of the transmission lines. The goals of this optimization, besides the impedance at 5.9 GHz and second harmonic is also to reduce as much as possible the  $S_{21}$  of the IMN which is directly related to the losses in the circuit. This will, indirectly, make the circuit as small as possible as well. The schematic and the results regarding the Output IMN can be seen in Figures 4.11 and 4.12, respectively.

Considering the impedance desired to be obtained,  $11.009 - j*16.946 \Omega$ , the result obtained with the schematic simulation is a satisfactory one with an impedance of  $11.375 - j*16.749 \Omega$  and the second harmonic impedance is also very close to the short circuit impedance as seen in Figure 4.12. As it will be seen later the impedance of the circuit using Method of Moments (MoM) simulation is not the same and so the circuit will have to suffer minor changes regarding length and width of the transmission lines.

### 4.6.3 Stability

Stability is a very important factor when designing a PA. In this case, it was decided that the Stability issues were addressed in the Input IMN, since the manufacturer also makes an example circuit board using this methodology. Considering this and the use of the  $50 \Omega$  resistor in the Input Bias Network, the other two aspects that can be used to reduce gain at lower frequencies are the use of a RC filter at the input, as well as a series resistor. This RC filter should contain a capacitor that is a short-circuit at the frequency of operation. The resistor is adjusted during the design to achieve a good stability factor and also *safe* stability circles. To better understand this changes and its results a description of the Input IMN is done in the next subsection.

### 4.6.4 Input IMN

Considering the approach in the previous subsection, it leads to the fact that, besides using the 3 stub approach as in the Output IMN, the RC filter another resistor must be used as well. Considering this and the Source Impedance, which is equal to  $3.557 - j36.505 \Omega$ , the same procedure as in the Output IMN was used, which is using the optimization techniques provided by ADS with limits for the width and length of the transmission lines. As in the Output IMN, the forward transmission coefficient is also an optimization goal, since it is important to reduce it as much as possible to avoid losses in the Matching Network. In the case of the Input IMN losses are more relevant due to the presence of resistors in the Matching Network. As a note the value of the resistor for the RC filter is  $22 \Omega$ .

With this being said, Figures 4.13 and 4.14 present the schematic used for this opti-



38



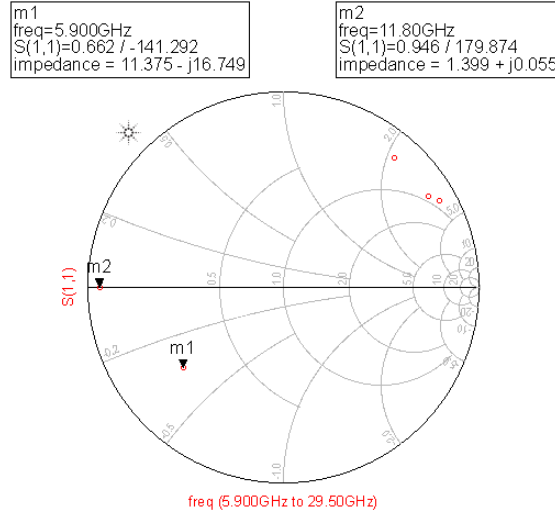


Figure 4.12: Output IMN Smith Chart

mization, as well as the Smith Chart with the impedance obtained, respectively.

As it can be seen in Figure 4.14, the impedances do not match as well as in the Output IMN. This is due to the fact that in this case the resistors were used as an ideal component, meaning that its impedance is the same for all frequencies. When doing this, the possibility of a perfect match is reduced as it is noted here. Besides this, the short-circuiting of the second harmonic is not achieved as well, even after several iterations of the optimization. As stated in the Output IMN subsection, these impedances are still not the final ones in terms of results since the MoM simulation will lead to different results and minor optimizations have to be done.

## 4.7 Minor Adjustments and Optimizations

In this section the changes regarding impedances obtained after performing minor tweaks in the transmission lines are shown.

First of all, both simulations use numerical approximations and thus they contain mistakes regarding real behavior. Nevertheless, when designing such circuit, these errors are normally small if the right procedures are used, which is the case of this design. Still, schematic simulation takes into consideration mathematical models for each type of trans-

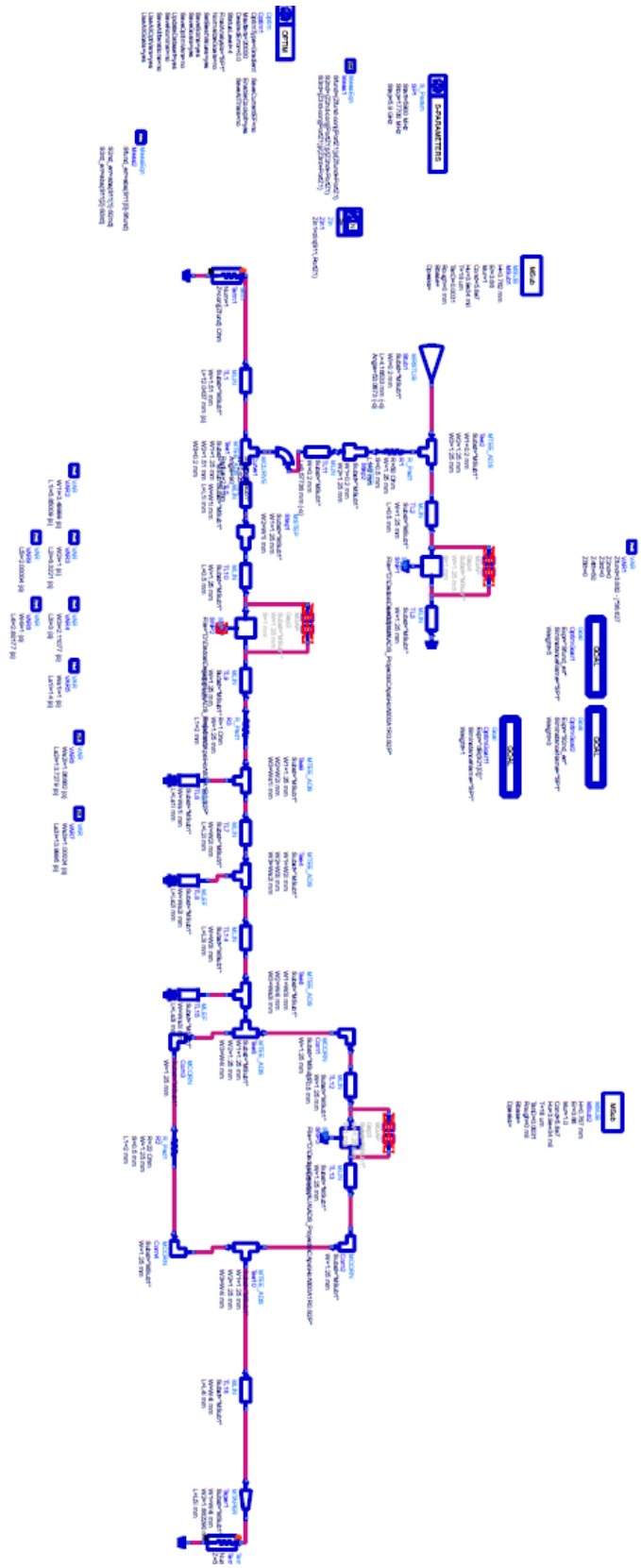


Figure 4.13: Input IMN Schematic

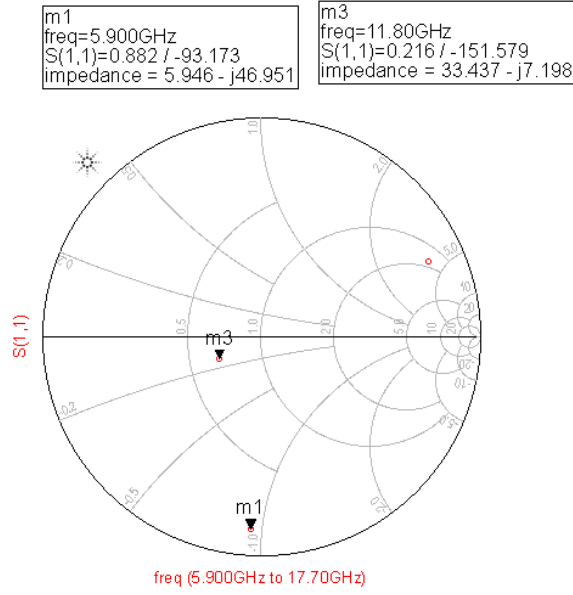


Figure 4.14: Input IMN Smith Chart

mission line (TLine, Open Stub, Short-circuit Stub, etc.) and in certain cases the interaction between such lines has a great importance to the design that it cannot be forgotten. In this cases, and to have a better approximation of the reality, MoM is used since it takes into account the Electromagnetic behavior of the different parts of the transmission lines and its influence on each other. This means that the impedances obtained using the schematic design will not be the same as the one obtained with the MoM simulation. So, why isn't the design made with MoM simulations from scratch? Well, MoM simulations are more complex and thus require more processing power and time, so the normal strategy is to start with a Schematic approach and then start iterating the MoM simulations to achieve the results desired.

In the particular case of this PA design, and as in the schematic procedure, the first IMN to be re-optimized was the Output IMN. Considering this and to better complete the Layout needed for the MoM simulation, the ground via was also added in the Bias Capacitor. Then, the procedure is simple: understand how each stub or transmission line influences the behavior of the impedance and change it iteratively according to that. As several iterations were done, only the final layouts for the Input and Output IMNs are shown in Figure 4.15.

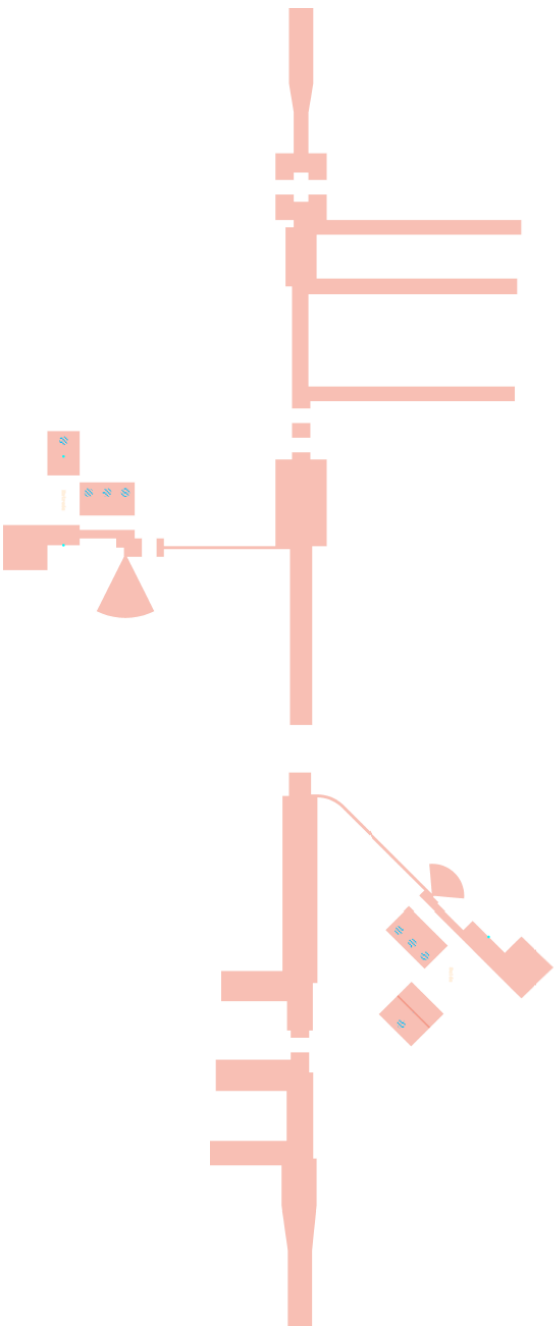


Figure 4.15: Final Layout without components - Left: Input Network; Right - Output Network

As it can be seen in the layout, three other capacitors were added for the reasons stated before. All the components are not present in Figure 4.15, but the space (including pads), is there so the layout is ready for design and assemble.



## Simulation Results

In this chapter the results of the simulations done are presented and evaluated according to the initial results using only ideal components.

### 5.1 1-Tone simulation with Ideal Components

The first simulation done was with only the impedances obtained with the Load-Pull characterization and the Source Impedance from the manufacturer at 5.8 GHz. This simulation was a one-tone simulation where a single tone is used to excite the PA. The setup can be found in Figure 5.1 and the results in 5.2.

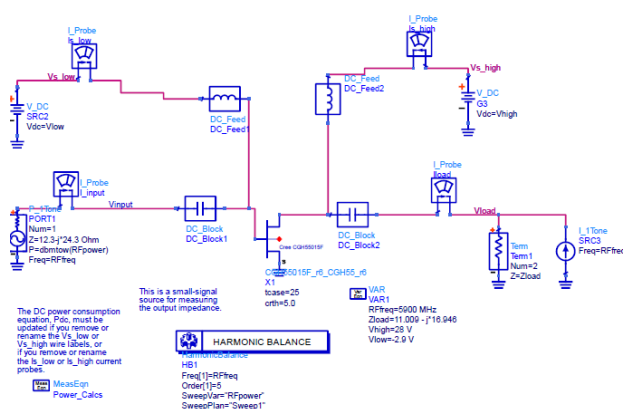


Figure 5.1: 1-tone Simulation with ideal components

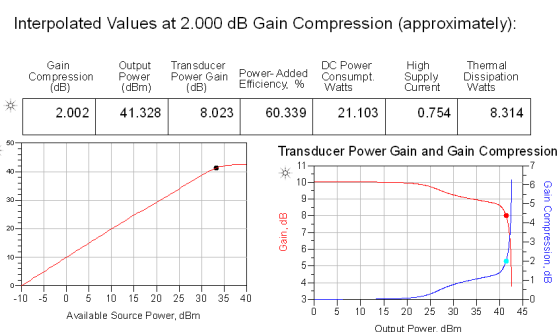


Figure 5.2: Results of 1-tone Simulation with ideal components

As it can be seen in Figure 5.2, the gain at 2dB compression point is about 8 dB with an Output Power of about 41 dBm and a PAE of 60%. At about 28.8 dBm of Output Power the gain is 9.3 dB and the PAE 14%.

This results serve only as a base for the evaluation done regarding the next steps in this design. As stated before the transmission lines and other components, such as resistors and capacitors, present losses for the whole circuit, which means loss in Output Power and, of course, gain.

## 5.2 1-Tone Simulation with MoM models

In this simulation the MoM models are used for a simulation closer to the reality. Nevertheless, two different tests were performed: one with a  $V_{GS}$  of -2.9V and the other with -3V. This was because with the  $V_{GS}$  of -2.9V the gain is closer to the original but the Output Power is lowered to about 38.5 dBm. Using -3V the gain drops to about 7.3 dB but the Output Power increases to 39.4 dBm. The PAE also suffers a slight difference: with -3V it is about 46% and with -2.9V it is about 44.9%. As a side note, all the values described are related to a gain compression of approximately 2 dB. Considering this, the best option will be better evaluated in the real system, since this change can provide an increase in the quality of the testing and final results.

The setup regarding this simulation is the layout presented in Figure 4.15 with the transistor connecting both layouts and all the other necessary components presented in the schematics. In terms of variable parameters, it works exactly the same way as the schematic presented in Figure 5.1. The results of this simulation with a  $V_{GS}$  of -2.9V can be found in Figure 5.3. Besides the values described above, the gain at an Output Power of approximately 29 dBm is about 9.2 dB and the PAE is 14%, which is a close result to the one presented in the ideal case.

## 5.3 2-Tone Simulation with MoM Models

The 2-Tone Simulation was done using a very similar setup to the one used for the 1-Tone Simulation. The main difference is the input signal given to the signal, which in this



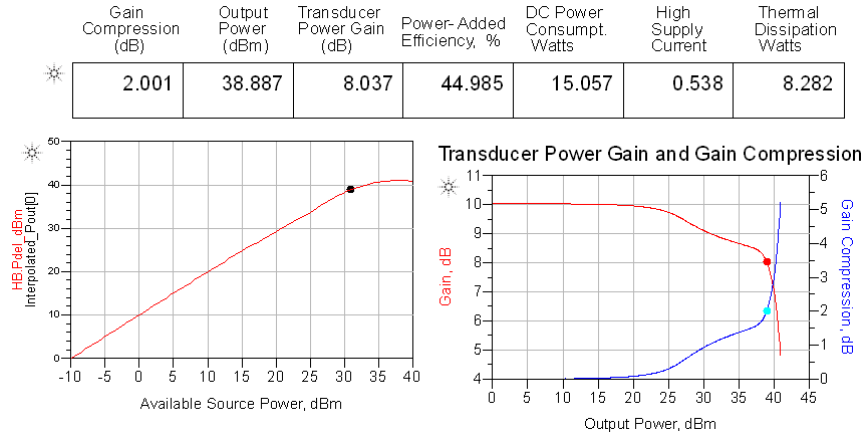


Figure 5.3: 1-tone Simulation Results

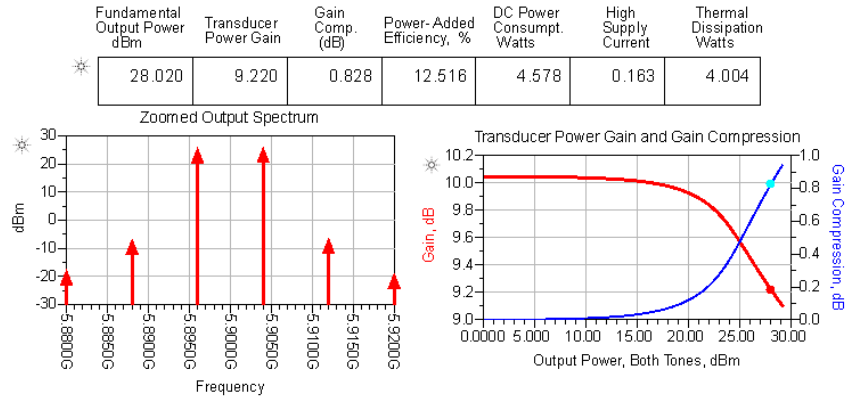


Figure 5.4: 2-tone Simulation Results

case is 2 Tones separated by approximately 8 MHz. This difference was selected because of the SEM of the IEEE 802.11p (review Table 2.1) and this test was to check if the PA was designed with a sufficient Bandwidth to allow this standard. Just as a remark, in this simulation both tones had the same power, which was the same as in the 1-tone simulation minus 3 dBm.

The results were very satisfactory and similar to the ones obtained with the 1-Tone simulation, apart from all obvious differences. Using a  $V_{GS}$  of -2.9V the Gain (at 2 dB compression point) was 8 dB, the PAE was 36.7% with an Output Power of 39 dBm. The results, at 28 dBm of Output Power can be viewed in 5.4.

Another characteristic that can be withdrawn from this type of simulations is the 3<sup>rd</sup>

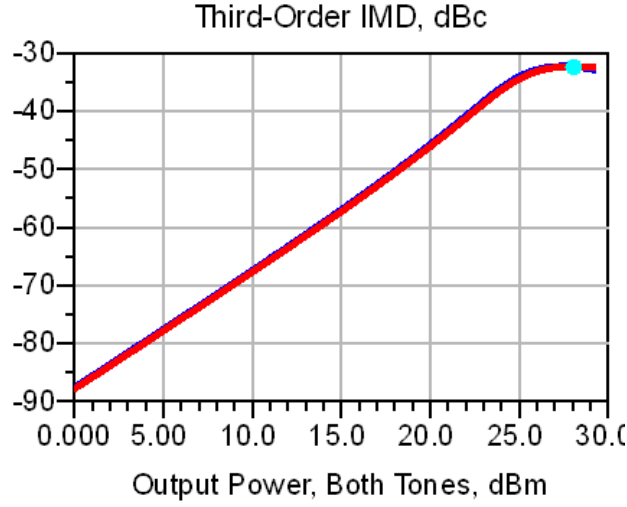


Figure 5.5: 2-tone Simulation Results

---

Order Interception Point. For this circuit, Figure 5.5 presents these results.

## 5.4 Stability Simulations

Using the same MoM models a stability analysis was performed, to confirm the theory explained in the design. Normally in the cases of PA design the most common points for oscillations are the lower frequencies, as stated before in Chapter 2.

Figure 5.6 shows that either  $\mu_{source}$  and  $\mu_{load}$  are greater than unity which means that the circuit is unconditionally stable and oscillations should occur. Nevertheless, when testing the designed PA precautions should be taken in order to prevent damage in components and instrumentation devices.

# Geometric stability factors $\mu_{\text{source}}$ and $\mu_{\text{load}}$

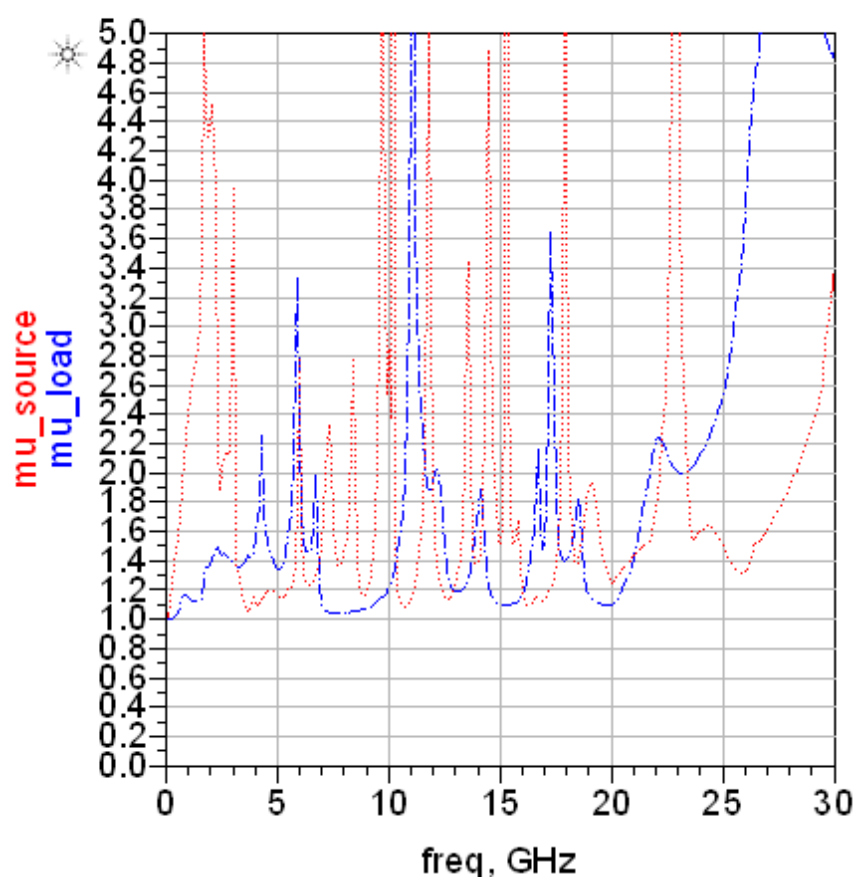


Figure 5.6: Stability Simulations



# Chapter 6

## Digital Pre-Distortion

### 6.1 Introduction

In this section the basic concepts behind Digital Pre-Distortion (DPD), such as Volterra Series and Memory Polynomials, are explained as well as the implementation used.

### 6.2 Why use Digital Pre-Distortion?

DPD is a Baseband compensation technique to, as the name says, compensate the non-linearities created by the PA, when it is operating close to peak-efficiency, that distort the signal. These distortions affect the clarity of the signal, as well as the possibility of keeping a certain signal in-band in terms of frequency [30]. Not being compliant with the bandwidth given for operation may result in the risk of violating laws that inhibit the use of such circuit. A generic DPD plus PA schematic is presented in Figure 6.1. and an example of how transfer functions influence the final result of the output signal can be found in Figure 6.2.

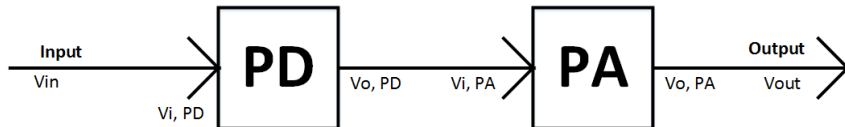


Figure 6.1: Schematic of DPD use with a PA

Backing off the PA is a solution for the distortions presented by itself. However, since efficiency is a prerequisite for Wireless Communications in mobile systems, that is normally

not a good way to face the problem. Adding to this, the production cost also increase significantly when using PAs that have larger output power than the one actually needed [31]. DPD is a solution that has gained traction in the RF world to address this problem in a more efficient way. DPD also has the advantage of allowing the "widespread deployment of Software Defined Radio (SDR) and also new network topologies involving tower top RF electronics" [31].

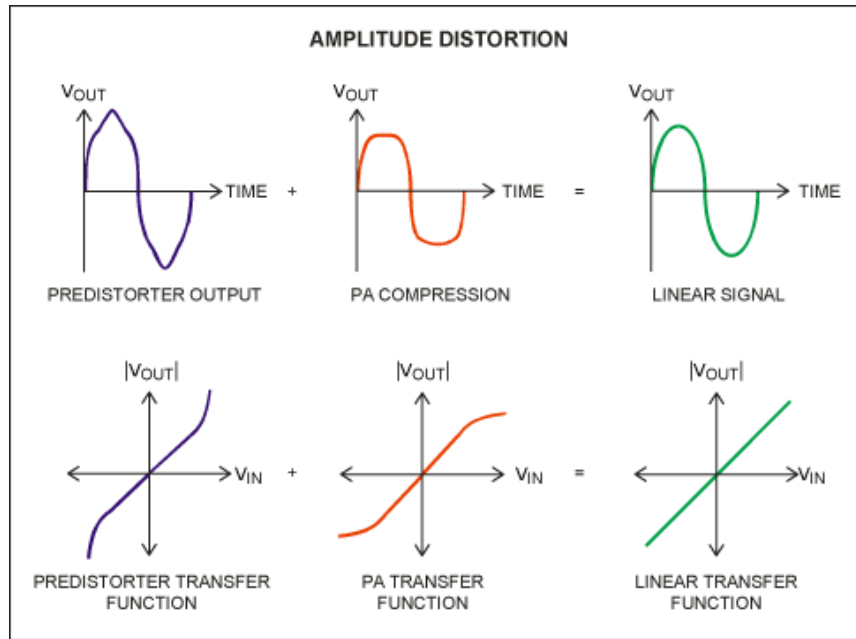


Figure 6.2: Example of the results produced by a PA using a DPD (Image taken from [32])

DPD techniques can have memory or be memoryless. What this memoryless technique means, is that it is considered that the non-linearities produced by PA are instantaneous and only these instantaneous non-linearities are trying to be compensated by an instantaneous DPD technique, which is characterized by the AM-AM and AM-PM curves seen in 3.

In order to fully explore the capabilities of DPD techniques, memory effects of the PA should be taken into consideration. This means that in order to characterize a PA a memory polynomial should be used, meaning this that the output of a PA at a certain moment in time, depends of the actual input and the previous inputs as well. Some examples of memory models for wide band DPD are Volterra series methods, and simpler cases like Wiener, Hammerstein, Wiener-Hammerstein and parallel Wiener structures [31].

### 6.2.1 Polynomial model with memory

Polynomial models are used to characterize the transfer function of a PA. This means that they can represent either the input-output relation of a RF signal or the input-output ratio of a band base signal which in the case of a DPD, makes more sense since DPD is done in base band. This input-output behavior can be seen in Eq. 6.1 [33].

$$x(t) = |\tilde{x}(t)| e^{j\theta(t)} \rightarrow y(t) = |\tilde{y}(t)| e^{j\theta(t)} \quad (6.1)$$

Volterra series provide a huge number of coefficients which makes its use unpractical. Nevertheless it is possible to obtain simplified expressions of such series like the memory polynomial described in Eq. 6.2 [31]:

$$y_{MP}(n) = \sum_{k=0}^{K-1} \sum_{m=0}^{M-1} a_{km} x(n-m) |x(n-m)|^k \quad (6.2)$$

In Eq.6.2, K represents the polynomial order and M represents the Memory of the Polynomial, x(n) represents the input signal of the system,  $y_{MP}(n)$  represents the output signal of the system and  $a_{km}$  represent the polynomial model coefficients.

This polynomial model can be used to model and describe the behavior of the PA. It is important to understand that the model description of the PA does not have to be perfect, but the pre-distortion linearization must be as good as possible. The memory polynomial presents a good option as it is capable of describing and modeling non-linear systems with good quality [34]. The expression presented in Eq.6.2 can be seen in a matrix form as shown in Eq. 6.3.

$$\begin{bmatrix} y(0) \\ \dots \\ y(n) \\ \dots \\ y(N-1) \end{bmatrix} = \begin{bmatrix} v_{10}(0) & \dots & v_{p0}(0) & \dots & v_{1Q}(0) & \dots & v_{PQ}(0) \\ \dots & \dots & \dots & \dots & \dots & \dots & \dots \\ v_{10}(n) & \dots & v_{p0}(n) & \dots & v_{1Q}(n) & \dots & v_{PQ}(n) \\ \dots & \dots & \dots & \dots & \dots & \dots & \dots \\ v_{10}(N-1) & \dots & v_{p0}(N-1) & \dots & v_{1Q}(N-1) & \dots & v_{PQ}(N-1) \end{bmatrix} \times \begin{bmatrix} b_{10} \\ \dots \\ b_{p0} \\ \dots \\ b_{1Q} \\ \dots \\ b_{PQ} \end{bmatrix} \quad (6.3)$$

In Eq. 6.3,  $v_{pq}$  is equal to  $x(n-q) \cdot |x(n-q)|^{p-1}$ , so the equation can be summarized

as  $Y = X \cdot B$ . Since both  $y(t)$  and  $x(t)$  are known, the goal is to obtain the coefficients  $B$ . In order to do so, Normalized Mean Square Error (NMSE) is used. The expression for obtaining vector  $B$  using NMSE is presented in Eq. 6.4.

$$B = (X^H \cdot X)^{-1} \cdot X^H \cdot Y \quad (6.4)$$

, where  $X^H$ , means the transposed complex conjugate of  $X$ .

### 6.3 Polynomial Model with memory of a Digital Pre-distorter (PD)

As it was seen before, the function of Digital PD, can be implicitly defined as,

$$F_{PD}(v_{in}) = F_{PA}^{-1}(G_0 \cdot v_{in}), \quad (6.5)$$

where  $F_{PD}$  is the transfer function of PD and  $F_{PA}$  is the function of a PA. However, and since PAs do not have a linear behavior, the transfer function of a PD cannot be obtained this way. This means, that in practice, the function of the PD has to be obtained experimentally, either, directly or indirectly. In the scope of this thesis, the direct learning method is the one used as it is simpler and easier to implement while having good results as well. In this case, the PD coefficients are calculated based on  $y(n)/G_0$  and  $x(n)$ , where  $G_0$  is the gain of the system PA+PD. The implementation can be briefly described by Figure 6.3.

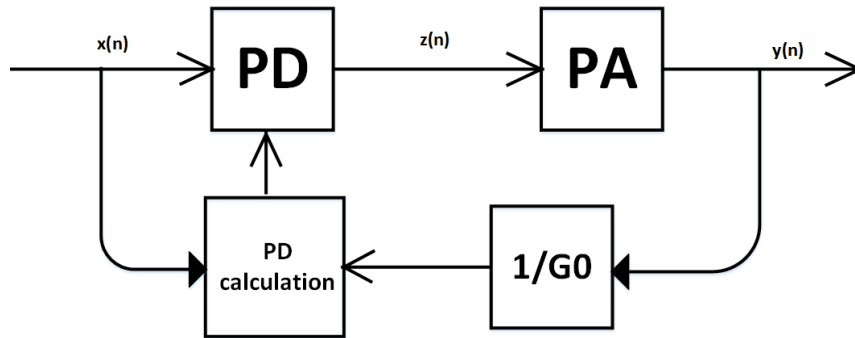


Figure 6.3: PD calculation using direct learning

In the next section the implementation using Matlab is explained, using a 16-QAM



signal with a 8 MHz bandwidth.

## 6.4 Polynomial model with memory of the Digital PD using Matlab

To implement a Digital PD in a real PA, measurements must be done to compute the coefficients of the PD using a known signal. As stated in the previous section the signal chosen is a 16-QAM signal with 8 MHz bandwidth. This signal has a bandwidth similar to the one from the IEEE 802.11p standard and the baseband modulation is also one of the possible modulation types of the standard, making this a good alternative for testing of the Digital PD.

The setup used for the measurements is shown in Figure 6.4. The driver PA must be used before the PA to increase the input power delivered to the PA designed, allowing the test of the PA up to higher power levels. The driver is a ZVE-8G+ from Mini-Circuits and uses a Voltage supply of 12 V, whereas the PA uses a  $V_{DS}$  of 28 V and a  $V_{GS}$  of -2.7 V. Other information about the driver amplifier can be found in [35]. This voltage is different from the one simulated since the DC current at -2.7V is closer to the 110 mA decided in the simulation than with -2.9 V. At the output of the PA, two attenuators of 10 dB each, are used to protect the VSA.

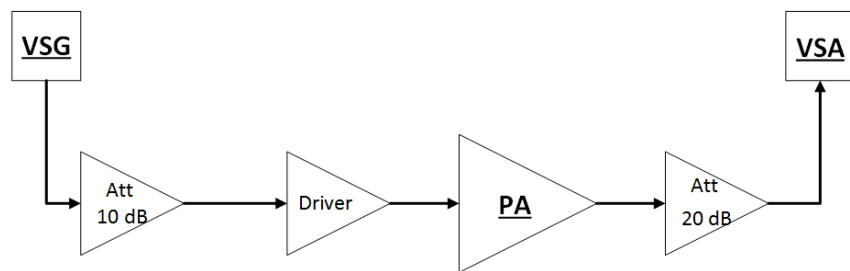


Figure 6.4: Setup used for measurements

After measuring the output signal for a certain input level, the PD coefficients can be calculated using the original signal and the measured signal that has a certain amount of distortion.

In order to calculate the coefficients the operational order is the following:

- Generation of a 16-QAM signal using Matlab and send it the Vector Signal Generator (VSG)
- Collect the signal from the VSA at the output of the PA
- Use the collected signal and the original 16-QAM signal to calculate the PD coefficients and the PD signal
- Send the PD signal to the VSG
- Collect the signal from VSA at the output of the PA
- Analysis of the results

The collected signal and the original signal must be synchronized in order to the algorithm to work. In order to do this, an auxiliary function is used which takes into account the correlation factor of both signals, aligns them and cuts the collected signal to the size of the original signal afterwards.

The coefficient calculation is first tested regarding Normalized Mean Square Error (NMSE) in Matlab with different values of M and K (memory and order of the polynomial). The graph containing that info can be found in Figure 6.5. The output power used for this was 28.8 dBm, since that is the maximum output power that can be used in IEEE 802.11p standard 2.1.

Having Figure 6.5 in consideration, the pair of values selected for the PD was  $K = 7$ ,  $M = 5$ . As the NMSE did not improve much when K and M were increased, and their increase implies greater simulation time and bigger complexity this pair means a good compromise between quality and simulation time. The results of the PD using a 16-QAM signal with 8 MHz bandwidth are presented in Figure 6.6.

## 6.5 DPD Results

As it can be seen from Figure 6.6, the improvement of the ACPR is about 20 dB comparing to the signal without PD, which means an increase in the linearity of the circuit. Apart from this, the average output power remains approximately the same, not reducing the PAE. Another fact is that, even though the linearity increases and the power

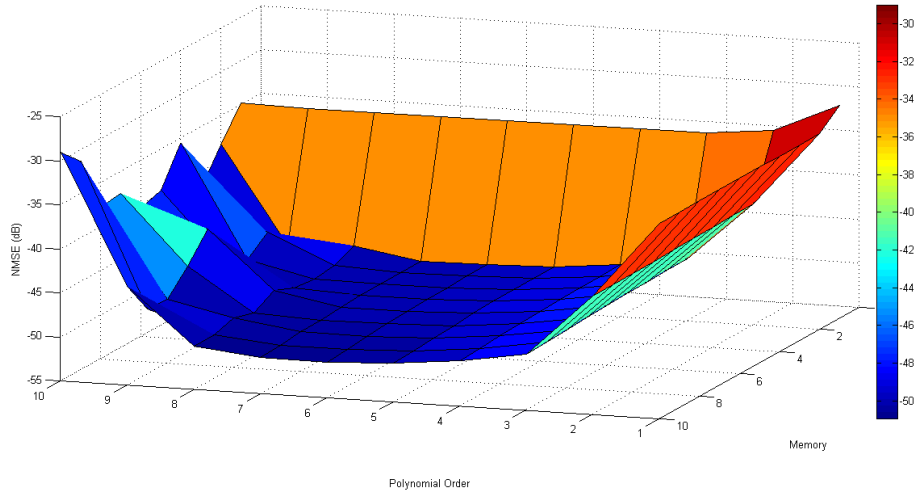


Figure 6.5: NMSE values for different memory and order polynomials

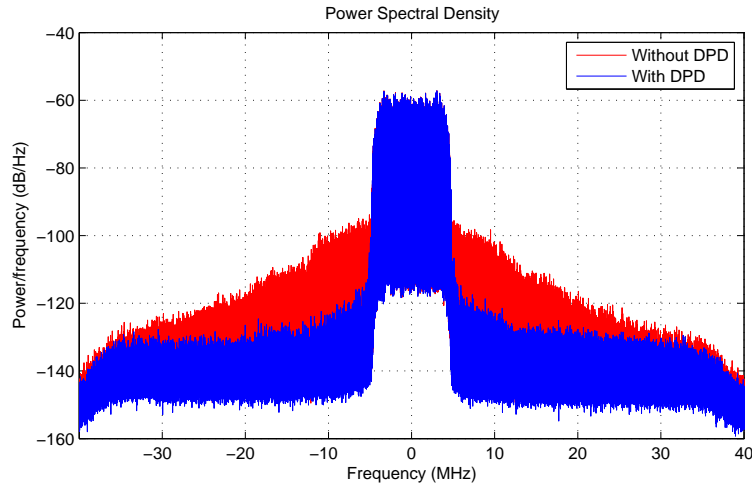


Figure 6.6: Comparison of a 16-QAM signal with PD and without PD at the output of the system.

output remains the same the PAPR of the signal increases with the DPD signal. The original signal had a PAPR of approximately 6.86 dB and the Predistorted signal had a PAPR of approximately 7.28 dB, resulting in an increase of approximately 0.4 dB. The Error Vector Magnitude (EVM) also decreases from 1.68% to 0.32% as it can be seen in Figure 6.7 and 6.8. The results can be considered satisfactory as it is proven that the PD is implemented correctly allowing the improvement of the signal conditions for transmission. The original signals also have a different look between each other. Although it seems the signal is of worse quality, the distortions introduced by the PD help the circuit to become

more linear when taking into account the non-linearities of the PA, as stated before. Figure 6.9 presents the difference between both signals.

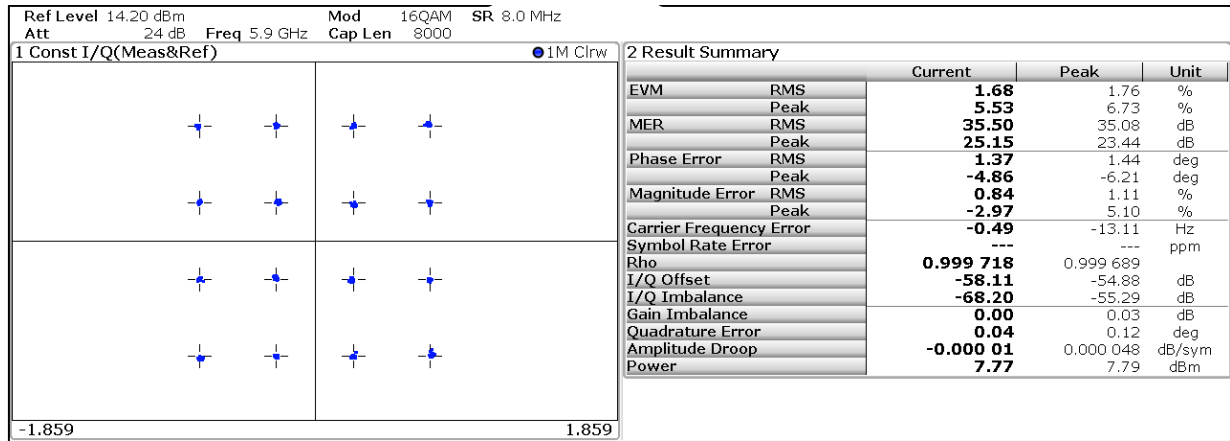


Figure 6.7: EVM analysis of a 16-QAM signal without DPD

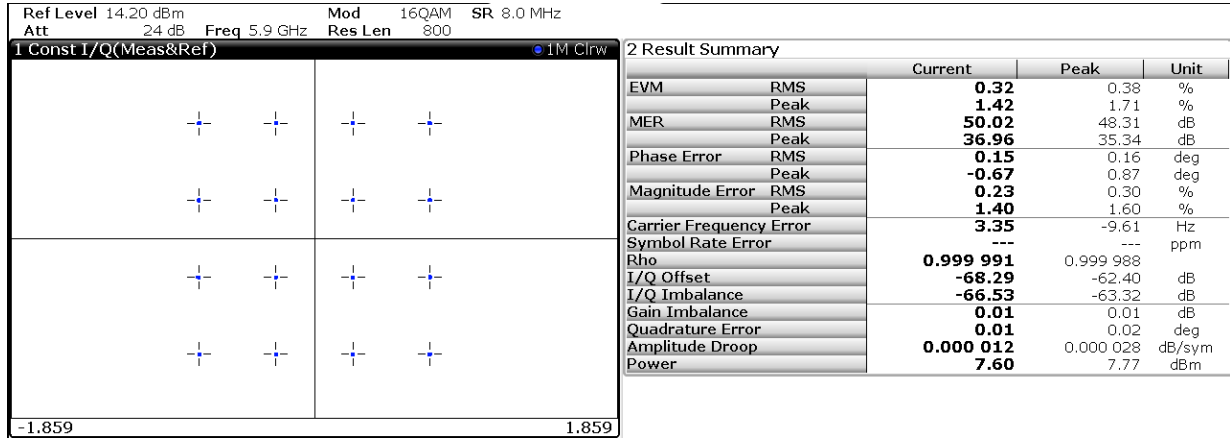


Figure 6.8: EVM analysis of a 16-QAM signal with DPD

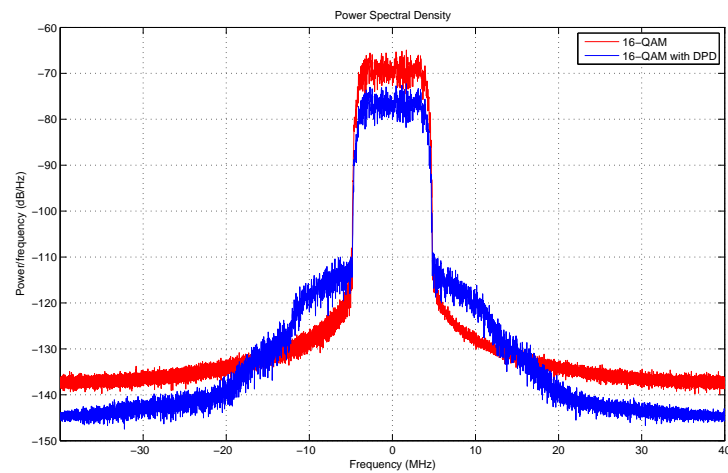


Figure 6.9: Comparison of a 16-QAM signal with PD and without PD before PA.



# Chapter 7

## Results

In this chapter Results are presented and discussed regarding the use of IEEE 802.11p signals with the PA designed and described in previous chapters.

### 7.1 Setup and PA built

The setup used is the same as the one used for the Digital PD, presented in the last section in Figure 6.4. The difference is the input signal used for the measurements. The PA designed can be found in Figure 7.1.

As it can be seen in Figure 7.1, some of the transmission lines were changed in order to increase the gain of the PA. In the original version of the PA the gain was of about 3 dB, very far from the projected value. In order to improve this value the width of the transmission lines was increased which would decrease the impedance of each line. Adding to this, a small stub before the RC filter in the input was added as well.

### 7.2 1-Tone Measurements

First of all it is important to know how does the PA behave in terms of PAE, output power and gain. For this, 1-tone simulations are an easy and simple way to do it. In order to know what is the input power the PA, measurements of the driver output power were made. This way the results of gain are more accurate than using the gain value given

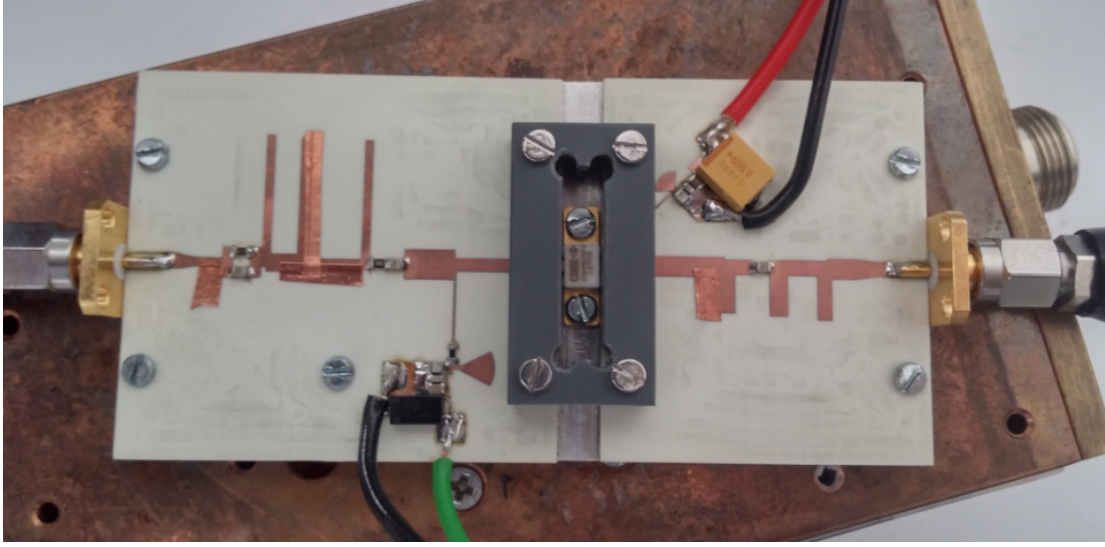


Figure 7.1: Class AB GaN HEMT PA for IEEE 802.11p applications - 5.9 GHz

in the data sheet of the driver. After that, the output power of the PA is measured and also the drain current is written down to allow PAE calculation. Figure 7.2 present output power, gain and PAE in the same graph to understand the relation between each other.

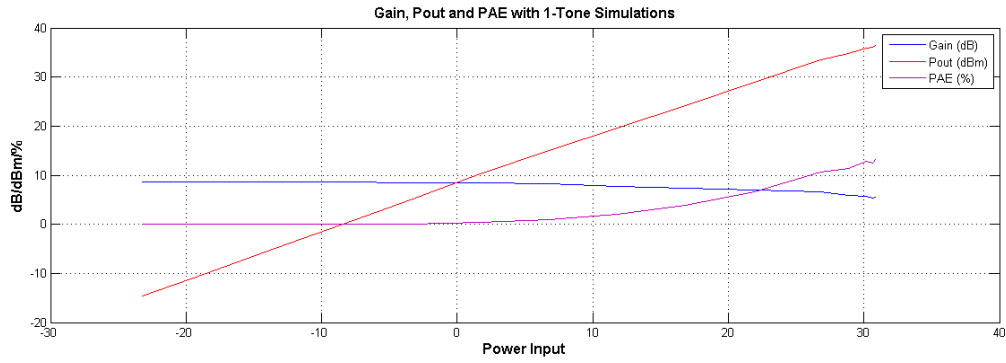


Figure 7.2: Gain, output power and PAE measurements

In Table 7.1 the characteristics in terms of output power, gain and PAE are compared between the simulated and obtained result.

As it can be seen from Table 7.1, the PA characteristics were changed which is normal. Nevertheless, these greater changes were produced by the alterations in the IMNs, that were made to improve the gain of the transistor. Although the saturation output power was not able to be calculated due to limitations in the output power of the driver (30



dBm), it seems that it should be around 37/38 dBm.

	<b>Output Power (dBm)</b>	<b>Gain (dB)</b>	<b>PAE (%)</b>
<b>Simulation</b>	38.887 (@ 2dB compression point)	8.037	44.985
<b>Experimental</b>	33.42 (@ 2dB compression point)	6.62	10.62

Table 7.1: Comparison between the simulated and the experimental results of the PA designed

As adjustments were made, another simulations was tried. This time, the adjusted transmission lines were measured and changed in the ADS simulation in order to try and understand why the changes were helpful. However, the results produced in the simulation were worse than the ones measured. This can be due to the fact that the copper lines added are not true microstrip lines and again there can be some issues with the accuracy of the transistor model.

### 7.3 IEEE 802.11p measurements

In order to use the setup assembled, a IEEE 802.11p signal must be sent by the VSG. To do that there were two options: either *produce* the signal using Matlab or using a preset signal of the same standard from the VSG. Since it was easier and safer to setup, the VSG option was selected.

After deciding the generation of the signal, the next step is to make an actual test to the circuit. With this being said, the first SEM to be tested was the one from power class C, as if this one is fulfilled, both A and B are also fulfilled. To confirm the achievement of this power class by the PA Figure 7.3 presents the SEM of the power class as well as the power spectrum of the signal at the output of the PA. To help understand what is the channel power Figure 7.4 shows the value for the same signal shown in Figure 7.3.

Achieving the power class C, automatically means that power classes A and B are also satisfied, since the power output needed for operation is lower (class A is 0 dBm and class B is 10 dBm) and SEM is less stringent than the one needed to operate in class C. With this being said, the final test needed is the power class D. The first test is without

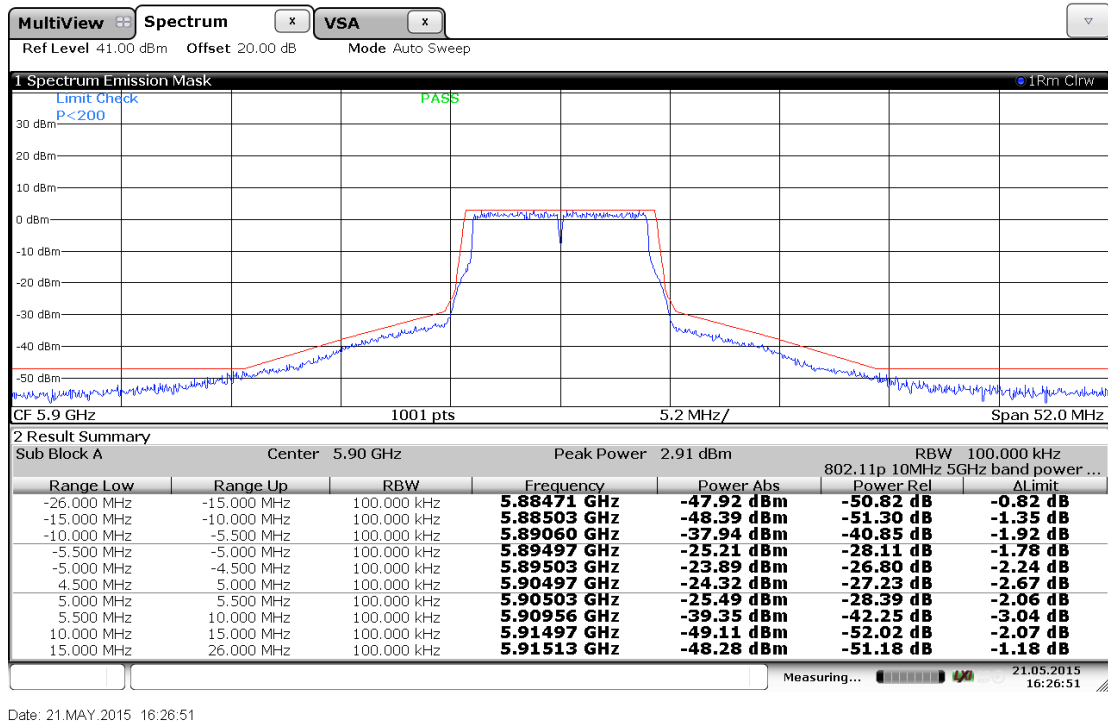


Figure 7.3: Power spectrum of the signal compared to SEM of power class C

PD and the SEM can be seen in Figure 7.5.

At this point, the use of the PD tested in the previous is a possible solution for this problem. However, there is a problem regarding this solution that does not allow the desired outcome. This problem is related to the quality of the signal produced. Since the signal produced by the VSG does not fulfill the SEM for the power class D and the PD adaptive algorithm takes into consideration the original signal and the signal at the output of the PA, the PD cannot improve the signal to a point where it is better than the original signal. With that being said, the PD implementation is tested for power classes C and D, where a small improvement is made in both cases. The power spectrum of the signals compared to the SEM of each power class can be found in Figures 7.6 and 7.7.

If Figures 7.3 and 7.6 are compared, slight improvements can be seen making the power spectrum more easily compliant with the SEM for the power class C. Unfortunately, power class D cannot be fulfilled as said before.

In the next section conclusions and future work is presented.

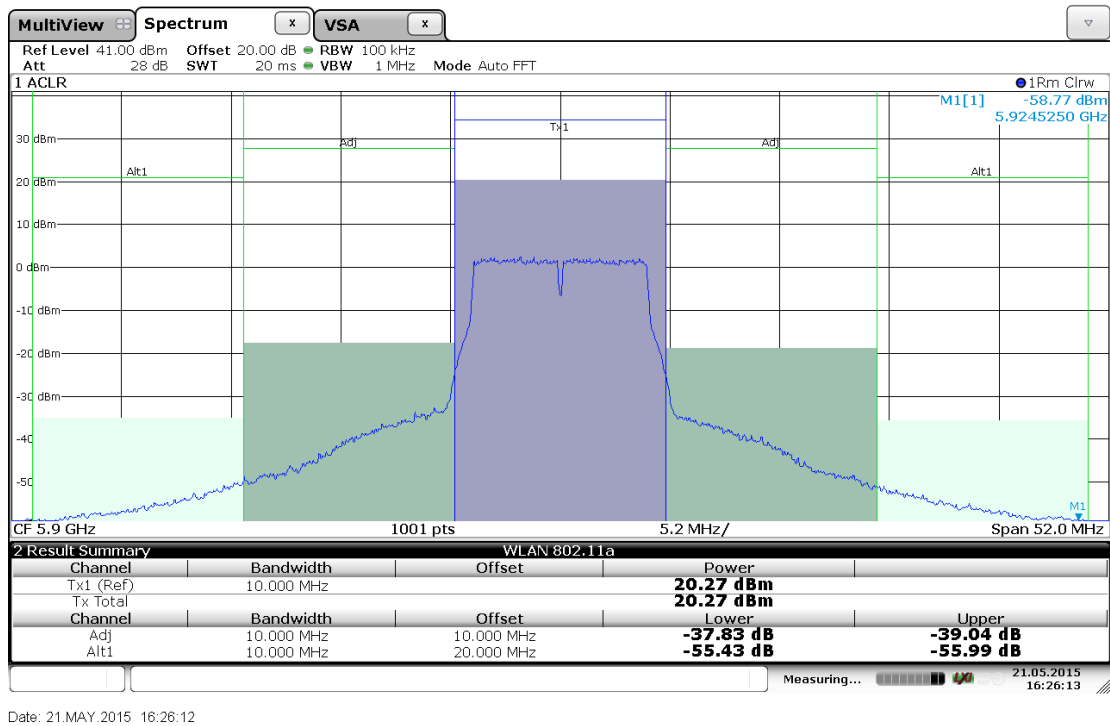


Figure 7.4: Channel power for the signal compliant with the SEM of power class C

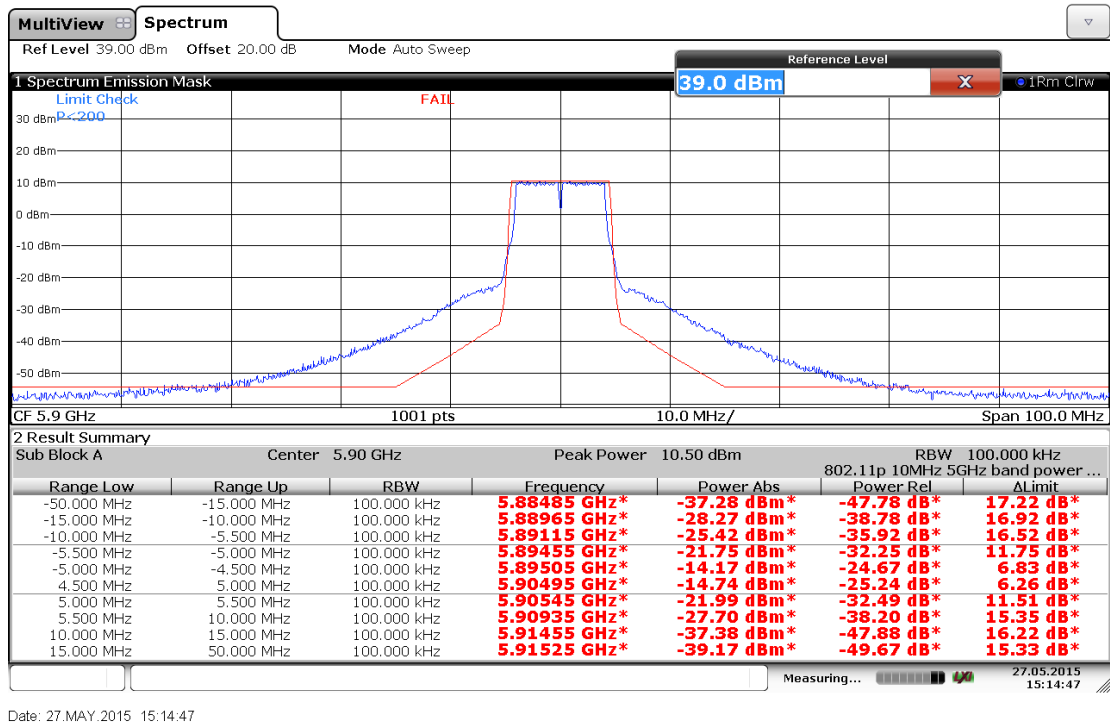


Figure 7.5: Power spectrum of the signal compared to SEM of power class D

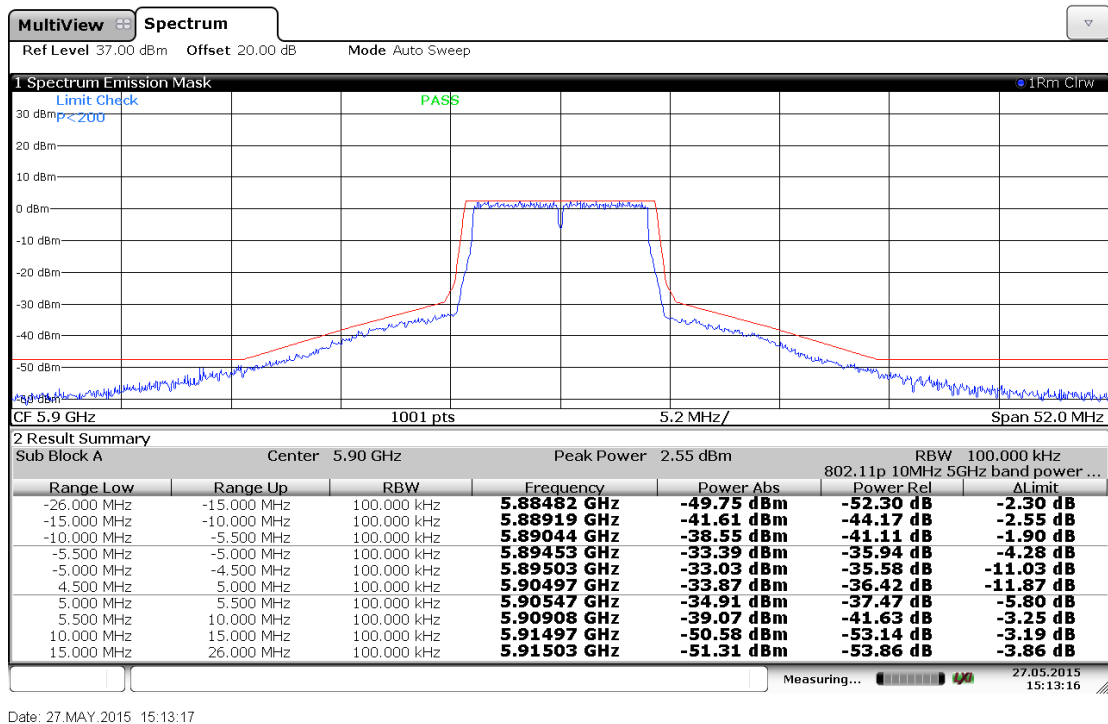


Figure 7.6: Power spectrum of the signal with PD compared to SEM of power class C

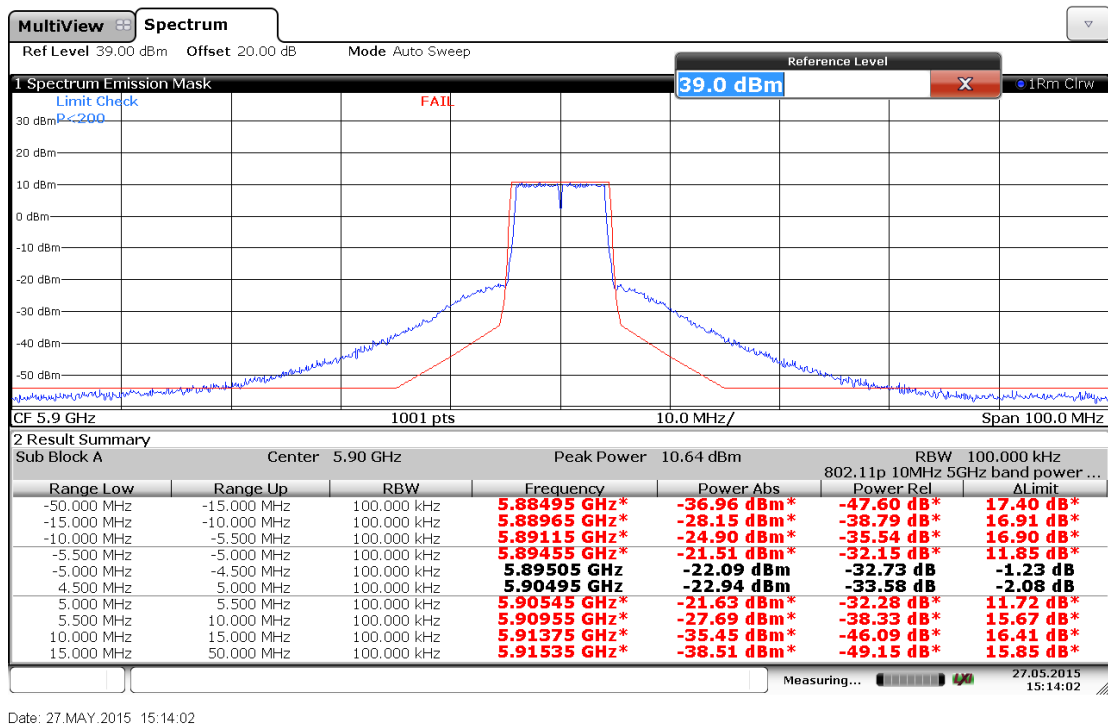


Figure 7.7: Power spectrum of the signal with PD compared to SEM of power class D

# Chapter 8

## Conclusions and Future Work

The goal of this chapter is to present a summary and conclusions of this dissertation as well as possible improvements to be made and possible options for future work.

### 8.1 Summary and Conclusions

During this dissertation it was possible to understand the importance of amplifiers, and specifically Power Amplifiers (PAs) in mobile communication systems, such as the vehicular communication systems, either for DSRC or ITS, as well as amplifiers' characteristics such as linearity and efficiency, and their importance to nowadays applications and concerns regarding environment protection. Besides the learning of the PA importance, the understanding of the use of the IEEE 802.11p standard for vehicular communications was also very important since vehicular communications are one of the future markets for mobile operators and other businesses.

With the goal of designing a PA that could be used in vehicular communications using IEEE 802.11p standard, first of all, the characteristics regarding PAs were studied, especially concepts like stability, linearity, efficiency and bias points/classes of operation.

In terms of classes of operation the main classes approached were A, AB, B and C, since those are the most common and most used in RF systems, since they represent the classes where the behavior of the amplifier is more linear. Using this knowledge, amplifiers were described taking into account, PAE, linearity, gain and output power.

After understanding the concepts cited before, the next step was to design a PA using for that purpose the software ADS from Keysight. All the steps necessary were followed, from the choice of the transistor and substrate for the PCB, going through the selection of the proper bias point for class AB operation, output and input Impedance Matching Networks (IMNs) designs and stability to build a PA as good as possible. Using ADS as Computer Aided Design (CAD) tool, it was possible to make better simulations of the PA, since electromagnetic simulations, using MoM, are more accurate than the schematic simulations, and also produce the sketches needed to produce the actual circuit.

Before testing the PA designed, a Digital Predistorter (PD) was designed to help achieve all the power classes allowed by the IEEE 802.11p standard for vehicular communications. First of all, a brief explanation of Digital Pre-Distortion (DPD) was done and then of the algorithm chosen and why, in this case the memory polynomial. This PD was tested using a 16-QAM signal with 8 MHz bandwidth, which is, in terms of baseband modulation and bandwidth, a similar signal to the one used in IEEE 802.11p.

Finally, to test the PA, a setup was done using a driver amplifier and the PA designed. With this, measurements regarding PAE, gain and output power were done to compare to the simulated results. As it was seen in the previous chapter, since the model is not a perfect representation of the real transistor, the simulated and experimental characteristics were different. Adding to this, some possible imprecisions of the PCB manufacturing can also contribute negatively for this changes. Another important point was the change of the transmission lines to improve the gain of the PA.

The other tests performed were with a IEEE 802.11p signal to check if the power classes were fulfilled. In the case of this design, only power classes A, B and C were fulfilled. Power class D was not fulfilled not even when using the PD designed, since the original signal does not possess enough quality to be able to produce a good result when using it to designed the Digital PD.

## 8.2 Future Work

To continue the development of this solution several paths can be taken.

One of them should be to try and generate a better signal of the IEEE 802.11p standard in order to be able to use the PD designed without needing to change the PA already designed and tested.

As the primary goal of this thesis was to implement a PA for vehicular communications, the PD came as an add-on to the thesis as a way to try and improve efficiency and reduce costs of production while aiming for the power class D of the IEEE 802.11p standard.

Another path that can be used to keep developing this work is to design one or two other highly linear amplifiers that can be introduced before the output stage amplifier designed in this thesis. This is a good approach, since transceivers normally have a very low output power, in the order of 0 dBm.

The Digital PD can also be improved and implemented in an FPGA and a DSP or simply an FPGA. This way, all the processing could be done in real-time allowing the deployment of this solution to the mass-market.





# Bibliography

- [1] <http://www2.lbl.gov/microworlds/alstool/emspec/emspec2.html>. Accessed: 17/04/2015.
- [2] Rabah Meraihi, Sidi-Mohammed Senouci, Djamal-Eddine Meddour, and Moez Jerbi. Vehicle-to-vehicle communications: Applications and perspectives.
- [3] M. Gramaglia, M. Calderon, and C.J. Bernardos. Abeona monitored traffic: Vanet-assisted cooperative traffic congestion forecasting. *Vehicular Technology Magazine, IEEE*, 9(2):50–57, June 2014.
- [4] National Instruments. [ftp://ftp.ni.com/pub/branches/uk/ats\\_2014/power\\_amplifier\\_testing.pdf](ftp://ftp.ni.com/pub/branches/uk/ats_2014/power_amplifier_testing.pdf). Accessed: 27/04/2015.
- [5] Matthew S. Gast. *802.11 Wireless Networks - The Definitive Guide*. 2002.
- [6] Rohde&Schwarz. [http://www.rohde-schwarz.de/file\\_12631/1ma152.2e.pdf](http://www.rohde-schwarz.de/file_12631/1ma152.2e.pdf).
- [7] [http://web.mit.edu/deweck/www/research\\_files/comsats\\_2004\\_001\\_v10/unit1%20success%20and%20failure/unit1\\_summary.htm](http://web.mit.edu/deweck/www/research_files/comsats_2004_001_v10/unit1%20success%20and%20failure/unit1_summary.htm).
- [8] F. J. Velez and R. Prasad. *WiMAX Networks: Techno-economic Vision and Challenges*. Springer, 2010.
- [9] Hannes Hartenstein and Kenneth P. Laberteaux. *VANET - Vehicular Applications and Inter-Networking Technologies*. 2010.
- [10] <http://mobiledevdesign.com/learning-resources/crystal-oscillator-psr-improves-80211n-evm-performance>. Accessed:27/04/2015.
- [11] Adão Silva and Atílio Gameiro. Wireless communications course from university of aveiro. Academic Year: 2015.

- [12] <http://www.maximintegrated.com/jp/app-notes/index.mvp/id/1849>. Accessed: 25/04/2015.
- [13] Guillermo Gonzalez. *Microwave Transistor Amplifiers*. 2 edition.
- [14] Hewlett Packard. S-parameter techniques for faster, more accurate network design, 1997.
- [15] Adel S. Sedra and Kenneth C. Smith. *Microelectronic Circuits*. 6 edition.
- [16] F.H. Raab, P. Asbeck, S. Cripps, P.B. Kenington, Z.B. Popovic, N. Pothecary, J.F. Sevic, and N.O. Sokal. Power amplifiers and transmitters for rf and microwave. *Microwave Theory and Techniques, IEEE Transactions on*, 50(3):814–826, Mar 2002.
- [17] Yong-Sub Lee, Mun-Woo Lee, Sung-Woo Jung, and Yoon-Ha Jeong. A high-efficiency sic mesfet power amplifier based on class-f configuration. *Microwave Conference, 2007. APMC 2007. Asia-Pacific*, pages 1–4, Dec 2007.
- [18] Diogo Manuel Pereira dos Santos Dias. Modelação e pré-distorção de um amplificador doherty, 2010.
- [19] Stephen A. Maas. *Nonlinear Microwave and RF Circuits*. 2 edition.
- [20] <http://www.ni.com/white-paper/13467/en/>.
- [21] José Carlos Pedro and Nuno Borges de Carvalho. *Intermodulation Distortion in Microwave and Wireless Circuits*. 2003.
- [22] Frederick Raab, Peter Asbeck, Steve Cripps, Peter Kenington, Zoya Popovic, Nick Pothecary, John Sevic, and Nathan Sokal. *RF and Microwave Power Amplifier and Transmitter Technologies — Part 1*. 2003.
- [23] <http://electronicdesign.com/test-amp-measurement/understanding-if-bandwidth-rf-signal-analyzers>. Accessed: 20/04/2015.
- [24] S. Kassim and F. Malek. Microwave fet amplifier stability analysis using geometrically-derived stability factors. In *Intelligent and Advanced Systems (ICIAS), 2010 International Conference on*, pages 1–5, June 2010.

- [25] A.R. Barnes, A. Boetti, L. Marchand, and J. Hopkins. An overview of microwave component requirements for future space applications. In *Gallium Arsenide and Other Semiconductor Application Symposium, 2005. EGAAS 2005. European*, pages 5–12, Oct 2005.
- [26] <http://www.cree.com/rf/products/28-v-telecom/packaged-discrete-transistors/cgh55015f1-p1>. Accessed: 17/06/2015.
- [27] [http://www.apc-productsplus.co.uk/index.php?route=product/product&product\\_id=97](http://www.apc-productsplus.co.uk/index.php?route=product/product&product_id=97). Accessed: 29/04/2015.
- [28] Abdullah AlMuhaisen, Peter Wright, J. Lees, P. J. Tasker, Steve C. Cripps, and J. Benedikt. Novel wide band high-efficiency active harmonic injection power amplifier concept. 2010.
- [29] J.C. McLaughlin and K.L. Kaiser. Deglorifying the maximum power transfer theorem and factors in impedance selection. *Education, IEEE Transactions on*, 50(3):251–255, Aug 2007.
- [30] George Vella-Coleiro. Improving the efficiency of rf power amplifiers with digital predistortion.
- [31] D.R. Morgan, Zhengxiang Ma, Jaehyeong Kim, M.G. Zierdt, and J. Pastalan. A generalized memory polynomial model for digital predistortion of rf power amplifiers. *Signal Processing, IEEE Transactions on*, 54(10):3852–3860, Oct 2006.
- [32] Tuning the max2009/max2010 rf predistorters for optimal performance - application note 4611.
- [33] E.G. Lima, T.R. Cunha, H.M. Teixeira, M. Pirola, and J.C. Pedro. Base-band derived volterra series for power amplifier modeling. In *Microwave Symposium Digest, 2009. MTT '09. IEEE MTT-S International*, pages 1361–1364, June 2009.
- [34] Lei Ding, G.T. Zhou, D.R. Morgan, Zhengxiang Ma, J.S. Kenney, Jaehyeong Kim, and C.R. Giardina. A robust digital baseband predistorter constructed using memory polynomials. *Communications, IEEE Transactions on*, 52(1):159–165, Jan 2004.
- [35] <http://194.75.38.69/pdfs/zve-8g.pdf>. Accessed: 17/06/2015.

